SKI Report 02:56

Research

Analysis of the Effect of UO_2 High Burnup Microstructure on Fission Gas Release

Lars Olof Jernkvist
Ali Massih

December 2002

ISSN 1104–1374
ISRN SKI-R-02/56-SE

SKI Perspective

Background and purpose of the project

During recent years a considerable amount of work has been performed on studying the behaviour of nuclear fuel at high burnup which has resulted in the generation of large amounts of data. One main finding is that the fission gas release is enhanced at high burnup. Therefore, the aim of this project was to investigate the mechanisms behind this behaviour of nuclear fuel. Another important aspect is the degradation of fuel thermal conductivity, which is analysed in this project. The analysis was performed using the computer code FRAPCON-3. In that way the capability of the code to model high burnup phenomena was assessed.

SKI has previously performed an evaluation of FRAPCON-3 (SKI Report 02.29).

Results

This project has contributed to the research goal of providing a basis for SKIs supervision by means of illustrating the problems of modelling nuclear fuel behaviour at high burnup. The project has also contributed to the research goal to develop competence concerning the licensing of fuel at high burnup, which is an important safety issue.

SKI project information

SKI ref.: 14.6-020614/02136
Responsible at SKI: Jan In de Betou

SKI Report 02:56

Research

Analysis of the Effect of UO_2 High Burnup Microstructure on Fission Gas Release

Lars Olof Jernkvist
Ali Massih

Quantum Technologies AB
Uppsala Science Park
SE-751 83 Uppsala
Sweden

December 2002

SKI Project Number 02136

List of contents

Summary

This report deals with high-burnup phenomena with relevance to fission gas release from UO_2 nuclear fuel.[1] In particular, we study how the fission gas release is affected by local buildup of fissile plutonium isotopes and fission products at the fuel pellet periphery, with subsequent formation of a characteristic high-burnup rim zone microstructure. An important aspect of these high-burnup effects is the degradation of fuel thermal conductivity, for which prevalent models are analysed and compared with respect to their theoretical bases and supporting experimental data.

Moreover, the Halden IFA-429/519.9 high-burnup experiment is analysed by use of the FRAPCON3 computer code, into which modified and extended models for fission gas release are introduced. These models account for the change in Xe/Kr-ratio of produced and released fission gas with respect to time and space. In addition, several alternative correlations for fuel thermal conductivity are implemented, and their impact on calculated fission gas release is studied.

The calculated fission gas release fraction in IFA-429/519.9 strongly depends on what correlation is used for the fuel thermal conductivity, since thermal release dominates over athermal release in this particular experiment. The conducted calculations show that athermal release processes account for less than 10% of the total gas release. However, athermal release from the fuel pellet rim zone is presumably underestimated by our models. This conclusion is corroborated by comparisons between measured and calculated Xe/Kr-ratios of the released fission gas.

[1] Part of this work was presented at the Enlarged Halden Programme Group Meeting, Storefjell Resort Hotel, Gol, Norway, September 8-13, 2002.

Sammanfattning

Denna rapport behandlar högutbränningsfenomen med betydelse för fissionsgas-frigörelse från kärnbränsle av UO_2.[2] I synnerhet studeras hur fissionsgasfrigörelsen påverkas av att klyvbara plutioniumisotoper och klyvningsprodukter byggs upp vid bränslekutsens periferi, med påföljd att en högutbränningsspecifik mikrostruktur bildas vid kutsens rand (rim zone). En viktig aspekt av dessa högutbränningseffekter är försämringen av bränslets termiska ledningsförmåga, för vilken vanligt förekommande modeller utvärderas och jämförs med avseende på teoretisk förankring och experimentellt underlag.

Dessutom analyseras Haldenprojektets högutbränningsexperiment IFA-429/519.9 med hjälp av beräkningsprogrammet FRAPCON3, i vilket vi inför modifierade och utökade modeller för fissionsgasfrigörelse. Dessa modeller beaktar förändringen av kvoten mellan Xe/Kr hos såväl den alstrade som frigjorda fissionsgasen med avseende på tid och rum. Vidare införs ett flertal alternativa korrelationer för bränslets termiska ledningsförmåga, och deras betydelse för den beräknade fissionsgasfrigörelsen studeras.

Den beräknade fissionsgasfrigörelsen i fallet IFA-429/519.9 beror starkt av vilken korrelation som används för bränslets termiska ledningsförmåga, eftersom termisk fissionsgasfrigörelse dominerar över atermiska processer i detta experiment. De genomförda beräkningarna visar att atermiska processer svarar för mindre än 10% av den totala fissionsgasfrigörelsen. Troligtvis underskattas dock atermisk frigörelse från bränslekutsens randzon av våra modeller. Denna slutsats styrks av jämförelser mellan uppmätt och beräknad Xe/Kr-kvot hos den frigjorda fissionsgasen.

[2] Delar av detta arbete har presenterats vid Enlarged Halden Programme Group Meeting, Storefjell Resort Hotel, Gol, Norge, 8-13 september, 2002.

1 Introduction

Fissioning of uranium and plutonium isotopes in uranium dioxide (UO_2) nuclear fuel produces about a hundred primary fission fragments, many of which are unstable and thus generate still other isotopes through their chains of decay. Among the most abundant fission products are the noble gases xenon and krypton. Most of these fission product gases are retained within bubbles and pores in the fuel material, but a certain fraction is released into the free volume of the fuel rod. This fission gas release (FGR) is a potential life-limiting phenomenon in nuclear fuel rods, since it gives rise to a build-up of rod internal gas pressure, which may eventually affect the fuel cladding integrity.

Several physical processes contribute to FGR in UO_2 nuclear fuel, and they are usually divided into athermal and thermal release mechanisms (Olander, 1976). Athermal release takes place by recoil and knockout of fission gas atoms by energetic fission fragments. Since only fission gas atoms located within a short distance (≈10μm) from a free surface can be released by these mechanisms, athermal release alone is not considered a potential problem for excessive fuel rod pressure buildup. In general, the recoil and knockout mechanisms result in release of less than 1% of the fission gas produced within the fuel pellets.

Thermal release mechanisms, however, have the potential for much larger release fractions. At fuel temperatures between approximately 1200°C and 1800°C, FGR results primarily from irradiation-enhanced diffusion of single gas atoms through the fuel material. Gas atoms within the UO_2 grains first diffuse to the grain boundaries, where the gas atoms accumulate in intergranular bubbles. These bubbles then successively grow and coalesce, eventually forming an interlinked flowpath through which the fission gas is vented to the rod free volume. This release mechanism is usually treated as a two-step process, where the second step leads to a delay, or incubation period, in the fission gas release. Both steps are complex processes, which are strongly affected by the fuel temperature, microstructure and fission rate. Additional thermal release mechanisms may come into play at temperatures above 1600°C. These high-temperature mechanisms, such as diffusion of gas bubbles or sweep-up of intragranular gas bubbles through grain growth, may be important under power ramps.

All the thermal and athermal fission gas release mechanisms outlined above are affected by changes in fuel rod properties with increasing burnup. In this paper, we attempt to identify high-burnup phenomena that, directly or indirectly, influence the fission gas behaviour in UO_2 fuel. Moreover, we study the relative importance of these phenomena by use of the FRAPCON3 fuel rod analysis program, which we apply to the Halden IFA-429/519.9 high-burnup fission gas release experiment.

The organization of the paper is as follows: Section 2 contains a brief survey of current knowledge, experimental findings and models for high burnup phenomena with relevance to fission gas behaviour in UO_2 fuel. In section 3, these phenomena are analysed and evaluated in light of numerical simulations. In particular, we consider thermal conductivity degradation and athermal fission gas release in the high-burnup fuel rim zone. Finally, in section 4, we analyse and discuss the fission gas behaviour in the Halden high-burnup experiment IFA-429/519.9.

2 High-burnup phenomena with relevance to FGR

One of the first major experimental programs directed towards fission gas release in high-burnup light water reactor (LWR) fuel was the international High Burnup Effects Program (HBEP), in which the fission gas release in altogether 82 well-characterized fuel rods with various designs and with rod average burnups in the range from 22 to 69 MWd/kgU were studied (Barner *et al.*, 1993). The main conclusion from the program was that the only mechanism for FGR that could be strictly related to high burnup was the formation of a characteristic microstructure at the pellet rim, which had the potential to enhance athermal FGR above a pellet average burnup of roughly 45 MWd/kgU. An upper-bound correlation, fitted to experimental data, showed that an increase in fractional FGR by at most 4% could be expected at a pellet average burnup of 80 MWd/kgU as a result of this rim zone effect. The results from HBEP gave impetus to further research on the nature of the high-burnup rim zone. This research, which is still ongoing, is surveyed and summarized below. The survey also includes research on other phenomena, such as thermal conductivity degradation of UO_2 fuel, which are known to indirectly affect FGR at extended burnup.

2.1 Fuel isotope distribution

As UO_2 nuclear fuel is taken into operation and subjected to irradiation, there is a successive change in the distribution of fissile material, power and fission products within the fuel pellets. In fresh fuel, the fissile material consists predominantly of ^{235}U, which is usually uniformly distributed in the fuel pellets. Hence, both power and fission products are generated with a relatively small variation along the fuel pellet radius. However, with increasing burnup, there is a non-uniform buildup of fissile plutonium isotopes through resonance capture of epithermal neutrons by ^{238}U and subsequent β-decays into ^{239}Pu and heavier fissile isotopes of plutonium (Duderstadt and Hamilton, 1976). Since the neutron capture takes place mainly at the pellet surface, the distributions of fissile material, fission rate and fission products will develop marked peaks at the pellet surface as fuel burnup increases. The shapes of these distributions are dependent not only on irradiation time, but also on the fuel initial content of ^{235}U, pellet radius and the neutron energy spectrum of the reactor. The properties of high-burnup fuel pellets are thus far more heterogeneous than in fresh fuel, which, together with the steep radial temperature gradient, complicates any modelling effort of the material.

With respect to fission gas release in high-burnup fuel, the non-uniform buildup of plutonium isotopes is important, since it is the underlying cause to the rim zone formation. However, the non-uniform distribution of fissile isotopes also affects the fission gas behaviour indirectly by altering the radial distributions of temperature, fission gas generation rate and gas composition. These indirect effects are further discussed in light of numerical analyses in section 3.

2.2 Fuel microstructure

2.2.1 Rim zone

The characteristic microstructure, which is observed close to the pellet surface in high-burnup fuel, is usually referred to as the 'rim zone structure'. This name is somewhat misleading, since the microstructure is related to enhanced local burnup and fission rate in combination with low temperature at the pellet rim, rather than to the radial position in itself (Turnbull, 2002).

Formation of the rim zone structure is characterized by reduction in grain size, increase in porosity and depletion of fission gas from the UO_2 matrix, (Matzke, 1995) and (Spino *et al*., 1996). The formation starts at a local burnup of 60-70 MWd/kgU by subdivision of grains at the fuel pellet outer surface and at pores and bubbles close to the surface. In early investigations, it was not clear whether this grain subdivision resulted from the local buildup of plutonium, or if it was a result of accumulated irradiation damage. From later studies on fuels with different initial enrichments, it is clear that the rim zone formation is due primarily to accumulation of irradiation damage, and not to the generation of plutonium (Kameyama *et al*., 1994) and (Kinoshita *et al*., 2000). At temperatures typically found at the pellet surface in LWR fuel, the formation starts at a local burnup of 60-70 MWd/kgU, irrespective of the plutonium concentration.

Initially, the grain subdivison occurs at both intragranular and intergranular positions, but later, the process is clearly concentrated to the boundaries of original grains. The concentration to grain boundaries is presumably a result of dislocation tangling at these sites, (Nogita and Une, 1994) and (Rest and Hofman, 1994). At a certain irradiation dose, tangled dislocations are organized into 20-30 nm subgrains (polygonization), which then act as nucleation sites for recrystallization. The fully recrystallized structure has a typical grain size of 200-300 nm, which is much smaller than that of the original material (≈10μm).

An alternative explanation to the grain subdivision is due to Thomas *et al*. (1992), who proposed that the fuel re-structuring was driven by stored energy of fission products in solution and in overpressurized gas bubbles. Although this explanation has been advocated also by later investigators, e.g. Spino *et al*. (1996), it seems to have less experimental and theoretical support than the hypothesis in which grain subdivision is triggered by dislocation tangling.

The recrystallized grains are depleted of fission gas, and the fuel matrix contains only a fraction (≈1/5) of the fission gas present within the large original grains, (Mogensen *et al*., 1999) and (Walker, 1999). Numerous measurements by electron probe micro-analysis (EPMA) have shown that the re-structured grains contain 0.20-0.25 wt% Xe. EPMA is a local technique, by which the amount of Xe, atomically dissolved in the fuel matrix and comprised in sub-nanometer sized intragranular bubbles, is measured within very small volumes of the material. With the X-ray fluorescence (XRF) technique, it is possible to measure the average gas content in larger volumes, which comprise gas also on grain boundaries and in pores.

By combining EPMA with XRF analyses, it has been shown that only a minor part (≈1/4) of the fission gas that is depleted from the grain matrix is released to the rod free volume during the grain re-structuring (Mogensen *et al*., 1999). The major part of the gas is trapped in newly formed, large-size (≈1μm) pores, which make the rim zone microstructure appear as cauliflower in micrographs. The rim zone porosity may reach 20 vol% and higher, but it is considerably lower in fuel that experiences mechanical restraint from pellet-clad mechanical interaction (PCMI). Hence, rim zone porosity above 10 vol% is rarely observed in fuel subjected to PCMI (Une *et al*., 2000).

The rim zone thus starts to form at the pellet outer surface when a local burnup of 60-70 MWd/kgU is reached. However, the progression of the re-structuring process and the propagation of the rim zone inwards can not be correlated to local burnup alone (Une *et al.*, 1997) Assuming that the re-structuring is triggered by accumulation of irradiation-induced dislocations, there will be a competition between dislocation production, which is controlled by local fission rate, and dislocation annealing, which is mainly controlled by local temperature. The inward propagation of the rim zone will thus be affected by the radial distributions of both fissile material and temperature (Manzel and Coquerelle, 1997). The exact threshold temperature, above which re-structuring of highly irradiated UO_2 will not occur, is yet unknown. However, observations on thermal recovery of defect clusters in UO_2 indicate that this temperature should be close to 850°C (Nogita and Une, 1994), and experiments are carried out within the international High Burnup Rim Project (HBRP) in order to resolve this issue (Kinoshita *et al*., 2000).

The re-structuring process is also influenced by the original grain size of the material. This could possibly be explained by the fact that the dislocation tangling that triggers grain subdivision takes place at grain boundaries (Nogita and Une, 1994). Large-grain UO_2 materials, with less grain boundaries per unit volume, thus have markedly higher resistance to re-structuring than small-grained materials (Une *et al*., 2000). It has been found that small, re-structured grains may coexist with original, untransformed grains up to a local burnup of 120 MWd/kgU. Above this burnup, the microstructure seems to be completely transformed (Walker, 1999).

The microstructural changes described above are believed to enhance athermal fission gas release in at least two different ways. First, it is assumed that part of the fission gases that is lost from the fuel matrix during the grain re-structuring is directly released to the rod free volume (Sontheimer and Landskron, 2000). The second assumption is that the usual athermal mechanisms for FGR, recoil and knockout, are enhanced by an increase in the specific surface (*S/V*) of the porous re-structured material (Bernard *et al*., 2002). However, according to several experimental observations, the rim zone porosity is not interconnected, and should therefore not significantly increase the fuel specific surface (Spino *et al*., 1996) and (Une *et al*., 1997). An alternative hypothesis to the increased fission gas release rate from the re-structured material is due to Lassmann *et al.* (2000), who recognized that irradiation enhanced athermal diffusion in the small re-structured grains is sufficiently fast to explain the observed matrix depletion of gas, and that the same mechanism could contribute to enhanced fission gas release from the rim zone.

In addition to the athermal release mechanisms described above, it should be recognized that the presence of a porous rim zone could have a strong effect on FGR under rapid power excursions, such as reactivity initiated accidents (RIA's). A rapid rise in fuel temperature could lead to fragmentation of the rim material due to excessive overpressure in the pores, and hence to a burst-like release of the fission gas inventory (Rest and Hofman, 1995), (Lemoine *et al*., 2000).

Finally, it should be mentioned that there is concern not only for enhanced fission gas release, but also for degraded thermal conductivity in the porous rim zone material. This is further discussed in section 3.4.

2.2.2 Intragranular gas bubbles

Fission gas atoms in UO_2 fuel have a tendency to precipitate into small (≈2-4nm) and immobile intragranular bubbles, in which they are trapped and thus hindered from diffusional transport to the grain boundaries (Lösönen, 2000). Consequently, a dense population of intragranular bubbles implies a reduced effective diffusion rate for gas atoms.

The concentration and size distribution of intragranular bubbles are primarily governed by the local fuel temperature and fission rate. However, experimental investigations have shown that there is a coarsening of intragranular bubbles with increasing burnup, which seems to occur more or less independently of temperature and fission rate (Kashibe *et al*., 1993).

The underlying mechanism behind this coarsening is not fully understood, but it indicates that the effective diffusion rate of fission gas in UO_2 increases with fuel burnup, and accordingly, that also thermal FGR is enhanced in high-burnup fuel. In computer codes for fuel rod analysis, the enhancement of thermal FGR with burnup is usually modelled by correlating the applied gas diffusion coefficient with burnup in an empirical manner, e.g. (Berna *et al*., 1997) and (Turnbull, 1999), but there are also other approaches (White, 1994).

2.3 Fuel thermal conductivity degradation

Thermal conductivity of UO_2 is a key parameter affecting the thermal behaviour of the fuel during reactor operation. In particular, the fuel temperature, thermal expansion, fission gas release and gaseous swelling are strongly influenced by the fuel thermal conductivity. For un-irradiated UO_2, there has been a number of investigations that have lead to a reasonable understanding of the involved phenomena and therefore have resulted into fairly accurate expressions for UO_2 thermal conductivity in the temperature range of 300 to 3000 K. We cite the works of Hyland (1983) and Harding and Martin (1989) and references therein for review and conclusions on this subject. The case for irradiated UO_2 is, however, different. This is partly due to the paucity of direct experimental data on conductivity and also to some extent owing to great complexity of the subject matter; see section 3.4. It is, however, well established that UO_2 thermal conductivity decreases with exposure during reactor operation. Lucuta *et al.* (1996) have reviewed the subject (to 1996) and have offered a "pragmatic" phenomenological approach to modelling thermal conductivity of irradiated UO_2 fuel.

An alternative approach for identifying the burnup dependence of fuel thermal conductivity has been the fitting of in-reactor measured fuel central temperature data to a hyperbolic expression for conductivity. Pursuing this course, we mention the works by Kosaka (1993) and Wiesenack *et al*. (1996). Also, we point out the efforts of Ohira and Itagaki (1997), who developed a hyperbolic-type correlation for burnup-dependent conductivity. Ohira and Itagaki's work is supported by fuel thermal diffusivity measurements on irradiated fuel and also verified against fuel central temperature data. Lanning *et al*. (2000) have evaluated the aforementioned conductivity models for applications in fuel rod thermal analysis.

2.4 Pellet-clad mechanical interaction

The combined effects of fuel pellet swelling and inward cladding creep will result in closure of the pellet-clad gap and onset of mechanical interaction after 2-4 years of reactor operation. Pellet-clad mechanical interaction (PCMI) can thus be viewed as a high-burnup effect, which affects the fission gas behaviour in several ways.

Firstly, PCMI inhibits thermal FGR by lowering the fuel temperature through an improvement of the pellet-clad heat transfer. Secondly, the propensity for intergranular bubbles to grow and coalesce, and thereby to form an interconnected flowpath for venting of fission gases to the rod free volume, is reduced by hydrostatic pressure in the fuel material, (Kogai, 1997) and (Kogai *et al*., 1988). The hydrostatic pressure results from PCMI and, in the hot central part of the fuel pellet, also from compressive thermally induced stress.

In-reactor measurements of rod inner gas pressure often show that gas pressure increases markedly under power reductions, (Mogensen *et al*., 1993) and (Nakamura *et al*., 1999). When reducing power, the fuel hydrostatic pressure from PCMI and thermal stress is relaxed and the fission gas in intergranular bubbles can be more easily vented. However, under ramp tests, the measured increase in rod pressure under power reductions may also be due to the fact that released fission gas is unable to reach the pressure transducer until power is reduced and the pellet-clad gap opens. Axial flow of gas in closed-gap fuel rods is known to be slow (Bråten and Minagawa, 1999), and the delay in pressure equilibration between the fuel rod active section and plenum must therefore be considered in evaluations of in-reactor pressure measurements under ramp tests.

3 Analyses of FGR at high burnup

3.1 The FRAPCON3 computer code

In this study, we have used the FRAPCON3 computer code to evaluate the fission gas release behaviour of high-burnup UO_2 fuel. This code is developed and used by the US Nuclear Regulatory Commission (NRC) for thermo-mechanical analyses of LWR fuel rods with UO_2 fuel under steady-state operational conditions and moderate power excursions (Berna *et al*., 1997). Version 3 of FRAPCON was released in 1997. In comparison with earlier versions, it has extended capability to model high-burnup phenomena, and has been assessed and validated with experimental data from 45 high-burnup fuel rods, covering rod average burnups up to 74 MWd/kgU. A large part of the experimental data base stems from instrumented fuel assemblies in the Halden reactor.

Among the new high-burnup models included in FRAPCON3 are the micro-burnup model for calculating the radial distribution of fissile material and power in high-burnup fuel by Lassmann *et al*. (1994), and the correlation for fuel thermal conductivity and its degradation with increasing burnup by Lucuta *et al.* (1996). The models for fission gas release in FRAPCON3 are fairly simple. Athermal fission gas release, including enhanced release from the fuel pellet rim zone, is calculated from an empirical correlation between fractional athermal fission gas release and the pellet average burnup.

Thermal fission gas release is calculated by solving the equation of diffusion

$$\frac{\partial c(r,t)}{\partial t} = D(t)\left(\frac{\partial^2}{\partial r^2} + \frac{2}{r}\frac{\partial}{\partial r}\right)c(r,t) + \beta(t) \qquad (1)$$

in an equivalent spherical grain with radius a. Here, c is the local concentration of intragranular fission gas (mole/m^3), D is the effective gas diffusion coefficient (m^2/s) and β is the gas production rate (mole/m^{3}s). Equation (1) is solved under the assumption of re-solution of gas atoms from the grain boundary back into the spherical grain (Speight, 1969), which yields the time-dependent boundary condition (Forsberg and Massih, 1985)

$$c(r=a,t) = \frac{\lambda b(t) N(t)}{2D(t)}. \qquad (2)$$

Here, λ is the re-solution distance from the grain boundary (m), b is the re-solution rate (1/s) and N is the amount of gas per unit area of the intergranular bubbles (mole/m^2). N will grow with time, and thermal fission gas release is assumed to take place when N reaches a saturation threshold for the surface gas concentration in intergranular bubbles. This saturation threshold, N_s, is in FRAPCON3 correlated to temperature, T (K), bubble radius, r_b (m), and fuel hydrostatic pressure, P_h (Pa), through the perfect gas law (Dowling *et al.*, 1982)

$$N_s = \frac{C_0 r_b}{T}\left(\frac{2\gamma}{r_b} + P_h\right). \quad (3)$$

Here, C_0 is a constant and γ is the fuel surface tension (J/m^2). Equation (3) is strictly valid only for steady state, since it is derived on the basis of equilibrium between the bubble gas pressure and the externally applied hydrostatic pressure.

Equations (1) and (2) are in FRAPCON3 solved under time-varying conditions through an algorithm, which is claimed to follow the work by Forsberg and Massih (1985), but in reality, the implemented algorithm differs significantly from their work. The most apparent difference is that the boundary condition in eq. (2) is replaced with $c(r=a,t)=0$ in the FRAPCON3 implementation. Moreover, the algorithm in FRAPCON3 was found unable to reproduce the empirical Halden criterion for onset of thermal fission gas release (Vitanza *et al*., 1979), and it was therefore replaced with the original algorithm by Forsberg and Massih. We also introduced a correlation for the gas diffusion coefficient proposed by Turnbull (1999). In addition, the fuel hydrostatic pressure in eq. (3), which in the FRAPCON3 model is set equal to the rod internal gas pressure, also includes the pellet-clad contact pressure in our implementation. A comparison between the standard FRAPCON3 model for thermal FGR and our modified version is shown in figure 1, where predictions of 1% fractional fission gas release are compared with the Halden criterion by Vitanza *et al*. (1979).

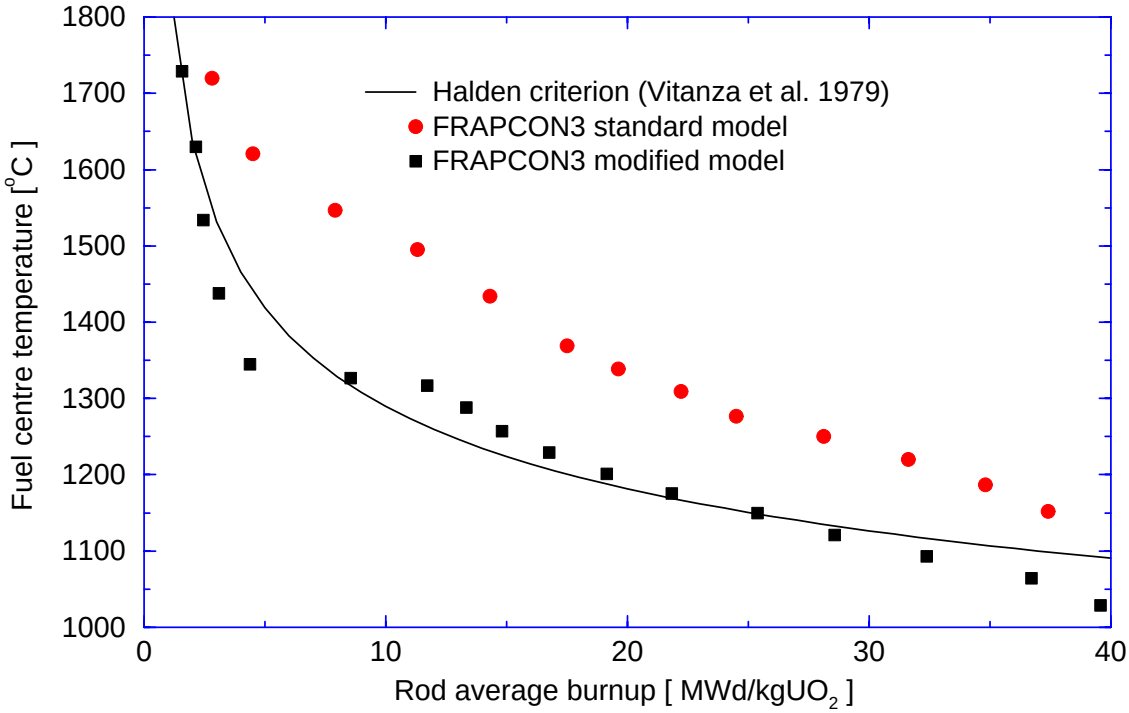

Figure 1: Predictions of 1% fractional fission gas release with the standard- and modified thermal fission gas release models in FRAPCON3. The predictions were made for a standard 17x17 PWR fuel rod with 4.5% initial enrichment; see table 1. The Halden criterion for onset of thermal fission gas release is shown for comparison (Vitanza et al., 1979).

Fuel pellets			**Cladding**		
Material		UO_2	Material		Zr-4
Density	%TD	95.0	Inner diameter	mm	8.36
Grain size	μm	10.0	Outer diameter	mm	9.50
Enrichment ^{235}U	%	3.0-4.5			
Pellet diameter	mm	8.19	**Fill gas**		
Pellet height	mm	13.46	Composition		He
Active fuel length	mm	3658	Gas pressure	MPa	2.5

Table 1: Design data on a standard 17x17 PWR rod, considered in analyses.

3.2 Distribution and composition of produced fission gas

The non-uniform buildup of fissile plutonium isotopes in the fuel pellets is reflected in the distribution of retained fission products at high burnup. Figure 2 shows the radial distribution of burnup at a pellet average burnup of 50 MWd/kgU, as calculated with FRAPCON3. Since the amount of produced fission gas is proportional to burnup, figure 2 also reflects the distribution of retained fission gas, provided that fission gas release has not occurred. The calculation was performed for a standard 17x17 PWR fuel rod with 3.5% enrichment of ^{235}U, which is subjected to through-life irradiation in a PWR. The rod design is detailed in table 1. In order to illustrate the influence of enrichment and reactor type on the radial burnup distribution, a calculation was also performed for an identical rod, but with 8.0% enrichment and the irradiation taking place in a heavy boiling water reactor (HBWR) instead of a PWR. This case is representative of typical test rods being irradiated in the Halden experimental HBWR. Although the micro-burnup model in FRAPCON3 is approximate, it is clear that the distributions of burnup and retained fission gas at the pellet periphery differ significantly for the two cases as a consequence of the differences in fuel enrichment and reactor neutron energy spectra. As further discussed in section 3.3, the differences in local burnup and retained fission gas at the pellet periphery must be considered when comparisons are made between rim zone fission gas behaviour in commercial LWR fuel rods and Halden reactor test rods.

The non-uniform buildup of plutonium can be used to trace the radial location in the fuel, from which released fission gas originates. As shown in table 2, the fractional yields of stable isotopes of Xe and Kr differ between ^{235}U, ^{239}Pu and ^{241}Pu, which are the dominant fissile isotopes in irradiated UO_2 fuel. Gas released from the plutonium-rich rim zone has therefore a higher Xe/Kr-ratio than gas released from the fuel centre, and the radial location where FGR takes place can thus be estimated by measuring the Xe/Kr-ratio of the released gas (Noirot *et al.*, 2000). In order to quantify this effect, models in FRAPCON3 were extended so that xenon and krypton could be treated as individual gas species under fission gas production and release. The stable isotopes of Xe and Kr shown in table 2 were considered, and their local production rates were correlated to the local fission rate and composition of fissile isotopes in the fuel pellet. Moreover, Xe and Kr were treated as individual gas species also in the gas release model, which made it possible to calculate the Xe/Kr-ratio of gas retained within grains, gas accumulated in grain boundary bubbles, and gas released to the rod free volume.

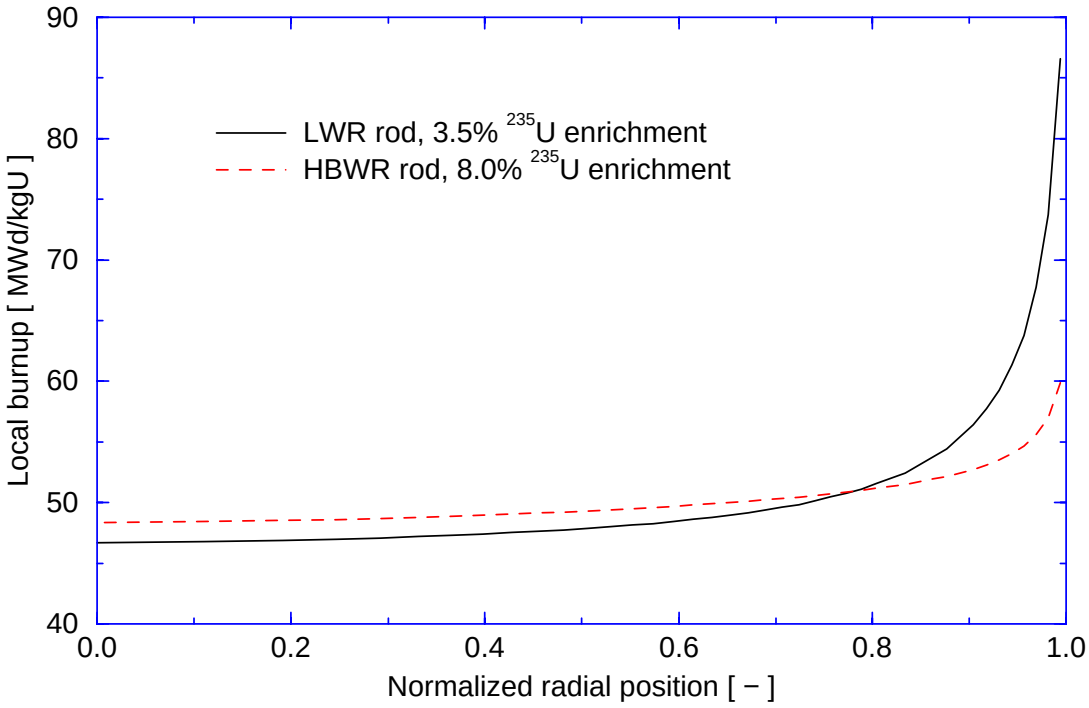

Figure 2: Calculated radial distribution of burnup in two fuel pellets, both with an average burnup of 50 MWd/kgU. A fuel rod design as specified in table 1, and a radial mesh consisting of 50 equal volume annuli were used in the analysis.

Stable isotope	**Fractional yields**		
	^{235}U	^{239}Pu	^{241}Pu
^{131}Xe	0.02887	0.03867	0.03067
^{132}Xe	0.04273	0.05263	0.04078
^{134}Xe	0.07749	0.07562	0.07599
^{136}Xe	0.06270	0.06940	0.06714
Total Xe	0.21179	0.23632	0.21458
^{83}Kr	0.00549	0.00288	0.00200
^{84}Kr	0.01006	0.00474	0.00350
^{85}Kr	0.00287	0.00130	0.00085
^{86}Kr	0.01964	0.00770	0.00606
Total Kr	0.03807	0.01662	0.01241
Xe/Kr	5.56	14.22	17.29

Table 2: Cumulative yields of stable isotopes of Xe and Kr. From the OECD NEA database through White (2000).

As an example, figure 3 shows the calculated ratio of stable Xe to stable Kr with respect to fuel radius in a standard 17x17 PWR fuel rod with 3.5% enrichment of ^{235}U and a pellet average burnup of 35 MWd/kgU. The rod, which is described in table 1, was operated at a low constant power of 20 kW/m, and consequently, only athermal fission gas release occurred. As evidenced by the figure, the Xe/Kr-ratio varies with radial position in the fuel as a consequence of the non-uniform distribution of plutonium. The plutonium-rich rim zone yields a significantly higher Xe/Kr-ratio than the central part of the pellet, in which there is also a significant contribution from fissioning of ^{235}U. Moreover, there are large differences in Xe/Kr-ratio between the fission gas that is currently produced, and the gas accumulated in the fuel grain matrix and on fuel grain boundaries. The produced gas reflects the plutonium distribution at the current burnup (35 MWd/kgU), and has therefore a higher Xe/Kr-ratio than the accumulated gas, which stems from the entire irradiation history.

Figure 4 shows the predicted evolution for the Xe/Kr-ratio of gas accumulated in the rod plenum, as a function of rod average burnup. For comparison, the Xe/Kr-ratio was also calculated on the assumption that gas release takes place exclusively from the pellet centre or periphery, respectively. For fuel rods operated at higher power or to higher burnup, our calculations show that the Xe/Kr-ratio of gas accumulated in the rod free volume evolves in a complex manner. The evolution of this ratio depends primarily on fuel design (initial enrichment), reactor type (LWR/HWR) and the applied power history. This is further illustrated in section 4.

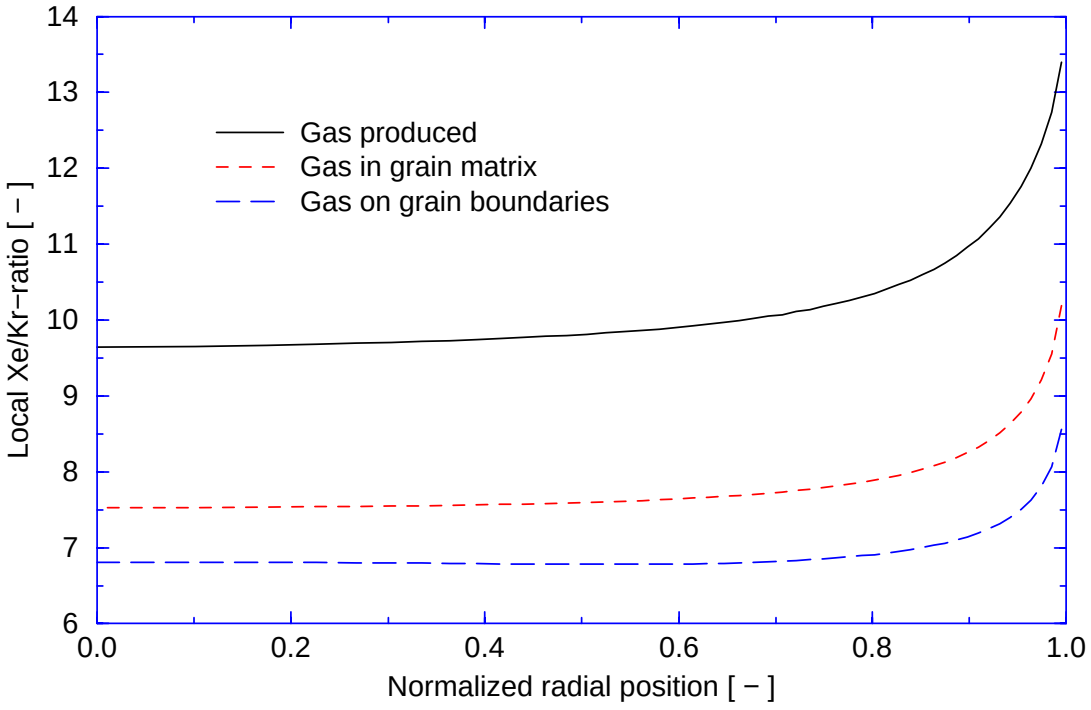

Figure 3: Local Xe/Kr-ratios of produced and retained fission gas at a pellet average burnup of 35 MWd/kgU, as calculated by FRAPCON3. The considered case is a standard 17x17 PWR fuel rod with 3.5% ^{235}U initial enrichment. The same fuel design and computational mesh as in figure 2 were applied.

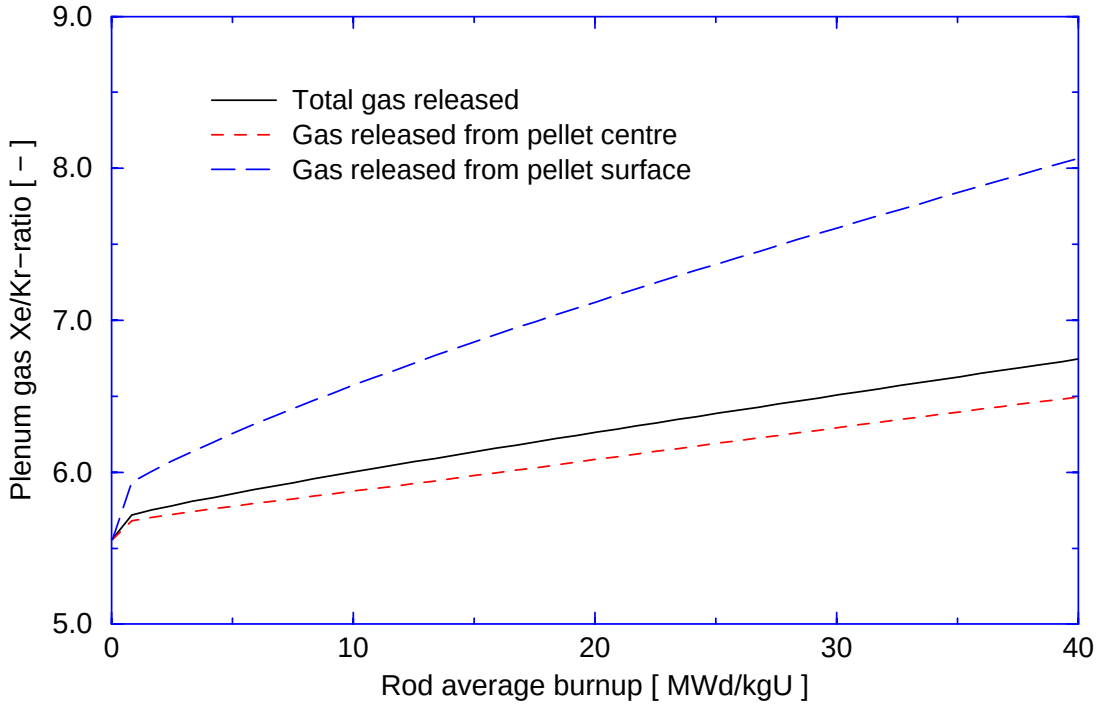

Figure 4: Calculated evolution of Xe/Kr-ratio for the rod plenum gas. For comparison, the Xe/Kr-ratio was also calculated on the assumption that gas release takes place exclusively from the pellet centre or surface, respectively. The same PWR rod as in figure 3 was considered in the calculations.

3.3 Rim zone gas release

As mentioned in section 2.2, the formation of a high-burnup microstructure in the pellet rim zone is associated with enhanced athermal fission gas release. In FRAPCON3, this enhancement is considered by assuming an additional contribution to the athermal release, when the pellet average burnup exceeds 45 MWd/kgU. The model is a purely empirical upper-bound correlation, which is based on experimental data from the HBEP (Barner *et al*., 1993).

An obvious weakness with this simple approach, in which the release is correlated to the pellet average burnup, is that the true radial distributions of burnup and fission product gases at the pellet rim are not considered. As shown in figure 2, these distributions can differ significantly between fuel rods with identical pellet average burnup. Models for rim zone fission gas release should therefore not be based on pellet average data, but formulated in terms of local properties in the rim zone. Such models have been proposed by several authors, e.g. (Bernard *et al.*, 2002), (Sontheimer and Landskron, 2000), (Lassmann *et al*., 2000) and (Forsberg *et al.*, 1994). These models are empirical, and are usually based on results from XRF studies of the re-structured fuel material in the rim zone. Such studies typically show that there is a decrease in retained fission gas concentration by approximately 25%, directly following the grain re-structuring at 60-70 MWd/kgU. Consequently, the major part of the accumulated fission gas inventory is not released during grain re-structuring, but trapped in the rim zone porosity.

After grain re-structuring, XRF studies indicate that the concentration of retained fission gas increases with burnup, but with a slower rate than expected in a situation where the total amount of produced gas is trapped within the fuel. Hence, part of the fission gas produced after grain re-structuring seems to be released to the rod free volume without significant delay.

Based on these observations, we have introduced a new model for rim zone athermal fission gas release in FRAPCON3. The model is locally applied, which means that for radial nodes located within the re-structured rim zone, a certain fraction of the fission gas production is directly vented to the rod free volume. The remaining gas is supposed to be trapped in the fuel porosity, and can later be released by thermal processes. From evaluations of fission gas release data from low-power LWR fuel rods at high burnup, the aforementioned release fraction was set to 0.30. Grain re-structuring is assumed to take place immediately, when the local burnup exceeds 65 MWd/kgU and the local temperature is below 900K. This is a simplistic treatment of the grain re-structuring, which in reality is a time-dependent process, controlled by a competition between production and annealing of crystal defects. The use of static thresholds for burnup and temperature should therefore be replaced by more elaborate modelling, as experimental data become available for the influence of temperature on rim zone formation (Kinoshita *et al*., 2000). Predictions from the new athermal fission gas release model are shown in figure 5 for the fuel rods described in section 3.2. The discrepancy in predicted high-burnup rim release between the LWR rods and the HBWR rod is explained by the differences in radial distribution of burnup and fission gas; confer figure 2. Also shown in figure 5 is the FRAPCON3 standard model for athermal fission gas release, which predicts identical release behaviour for the considered rods.

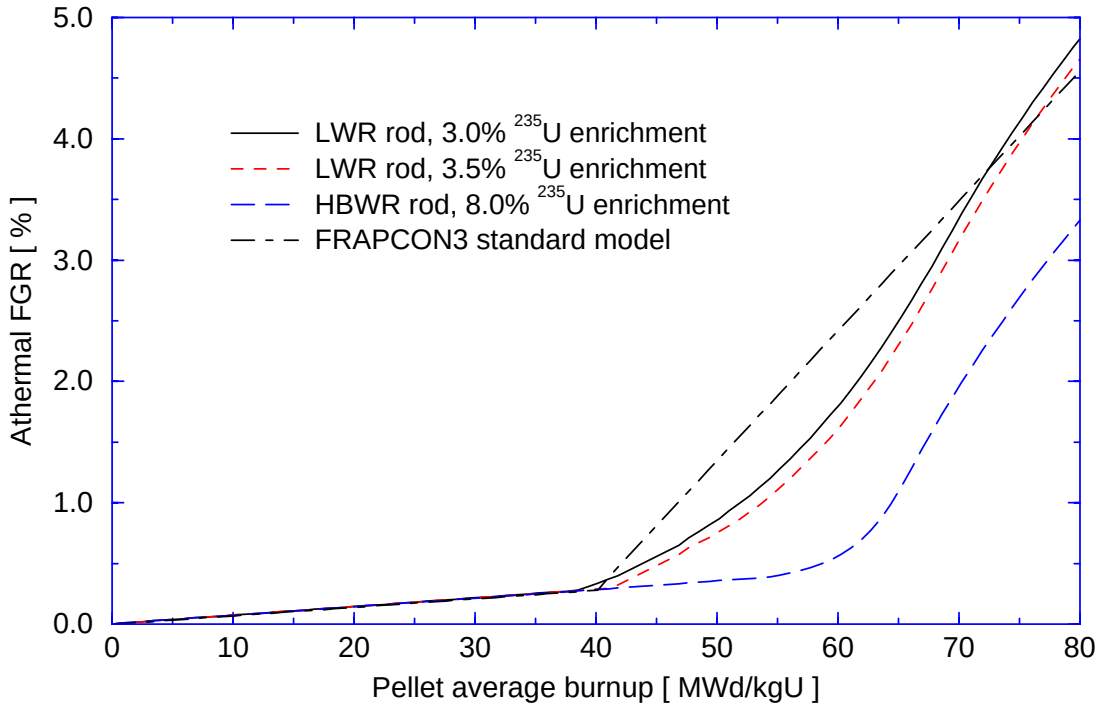

Figure 5: Athermal FGR for two typical LWR fuel rods and a typical test rod in the Halden HBWR, as predicted by the rim zone model described in section 3.3. Predictions from the FRAPCON3 standard model for athermal FGR are shown for comparison. The same fuel design and computational mesh as in figure 2 were applied.

3.4 Fuel thermal conductivity

3.4.1 Fuel temperature distribution

The steady-state temperature distribution $T(r)$ in a circular cylinder with a heat source, such as a nuclear fuel pellet, is described by the heat conduction equation

$$\frac{1}{r}\frac{d}{dr}\left(rk\frac{dT}{dr}\right) + q''' = 0, \tag{4}$$

where k is the fuel thermal conductivity and q''' is the volumetric heat generation rate. The thermal conductivity is a function of temperature, and it also depends on fuel porosity and impurities, which evolve during irradiation. The heat source q''' depends on the radial position r, and evolves during irradiation due to consumption of ^{235}U and production of fissile Pu isotopes, as discussed in section 2.1. The local energy production (burnup), denoted by $u(r)$, thus enters both the expressions of thermal conductivity, $k = k(T,u)$, and the heat generation rate, $q''' = q'''(r,u)$. Hence, integration of eq. (4) between the pellet centre (inner radius, r_0) and the pellet surface (outer radius, r_p) gives

$$\int_{r_0}^{r_p} k(T,u)\frac{dT}{dr}dr = -\int_{r_0}^{r_p}\left(\int_0^r q'''(r',u)r'dr'\right)\frac{dr}{r}. \tag{5}$$

This equation can be numerically solved for T, provided that k, q''', u and the pellet surface temperature are known quantities. The volumetric heat generation rate may be expressed in the form

$$q''' = \overline{q'''}\sum_j \alpha\sigma_{f,j}N_j(r,u)\phi(r), \tag{6}$$

where $\overline{q'''}$ is the radial average heat generation rate, $\sigma_{f,j}$ is the microscopic fission cross section for isotope j, $N_j(r,u)$ is the concentration of fissile isotope j at the position r and the burnup u, $\phi(r)$ is the thermal neutron flux, and α is a proportionality factor. The sum in eq. (6) is over all the pertinent fissile isotopes. For example, for monoenergetic thermal neutrons, $\phi(r)$ can be described by $\phi(r) = I_0(\kappa r)$ in a solid fuel pellet (r_0=0). Here, κ is the inverse neutron diffusion length (of the order of 2-3 cm^{-1}) and $I_0(\kappa r)$ is the zeroth order modified Bessel function. The fissile isotope concentration $N_j(r,u)$ can be determined as a function of irradiation time by neutron physics computations.

The problem here is the evaluation of the integrals in eq. (5) for determining fuel temperature. The right-hand side of eq. (5) involves the generation of fissile isotopes across the fuel during irradiation through relation (6). Simplified semi-empirical models have been developed to calculate eq. (6) by e.g. Palmer *et al*. (1983) and Lassmann *et al*. (1994) with a fair level of accuracy. The uncertainty on the left-hand side of eq. (5) is, however, larger than that of the right-hand side, since the precise nature of the fuel thermal conductivity $k = k(T,u)$, during irradiation, is not yet well established.

There have been two approaches to this issue. In one approach propounded by Lucuta *et al.* (1996), the thermal conductivity of UO_2 fuel is a combination of multiple effects. In particular, they write

$$k = k_0\, k_{1d}\, k_{1p}\, k_{2p}\, k_{3x}\, k_{4r}\,. \qquad (7)$$

Here, k_0 is the thermal conductivity of un-irradiated UO_2, which is a sum of a lattice term and a polaron term, and assumed to be well-established (Harding and Martin, 1989). k_{1d} describes the effect of the dissolved fission products, k_{1p} accounts for the precipitated fission products, k_{2p} is the porosity/bubble contribution, k_{3x} refers to the dependence on fuel stoichiometry, and k_{4r} describes the influence of radiation damage (vacancies, interstitials, dislocations, *etc*.) of the UO_2 lattice. For each of the irradiation-dependent factors appearing on the right-hand side of eq. (5), Lucuta *et al*. (1996) provide correlations, which are for the most part developed by fitting of available measured data, however certain deliberations have been given to their theoretical (generic) validity. These correlations are defined in appendix A.

The experimental data considered by Lucuta *et al.* include measurements on both irradiated nuclear fuel and laboratory produced simulated fuel specimens (SIMFUEL), that supposedly replicate the composition and microstructure (without fission gases and volatiles) of irradiated fuel. The "real" fuel data comprise both in-reactor measurements of central fuel temperature, from which k can be estimated via eq. (5), and post-irradiation thermal diffusivity measurements. To deduce a burnup-dependent thermal conductivity correlation from in-reactor central temperature measurements (an inverse method), we need an accurate calculation of the fuel surface temperature, which is affected by the uncertainty of the pellet-clad gap conductance. The post-irradiation conductivity measurements of fuel, as noted by Lucuta *et al*. (1996), are done after a certain period of cooling (usually more than a year), during which additional radiation damage from decay of certain actinides alter the thermal properties of the fuel. Moreover, post-irradiation measurements are affected by precipitation of fission products that were dissolved in the fuel lattice during fuel operation.

In an alternative approach for inferring the thermal conductivity of irradiated UO_2 fuel, one evades the individual phenomenological contributions that cause the degradation of thermal conductivity during irradiation by introducing a burn-up (and temperature) dependent term or function $h(u,T)$ in the lattice term of thermal conductivity, *viz.* $k_{latt} = (a + bT + h(u,T))^{-1}$ with a and b being constants and $h(0,T) = 0$. For example, Wiesenack *et al.* (1996) choose an empirical expression of the form $h(u,T) = (c_1 + c_2 T)u$, with c_1 and c_2 being constants, and use the left-hand side of eq. (5) to validate the central temperature data on reactor fuel obtained from the Halden heavy water BWR. Although an empirical based correlation may be appealing due to its simplicity, its validity would be confined to the particular set of data it rests on. Hence, prudence should be exercised when applying such a correlation for analysis of another type of reactor, e.g. fuels in modern commercial PWR's or BWR's.

3.4.2 Rim zone properties

An issue worth conferring is the impact of material re-structuring at the pellet rim, which occurs at high burnup (see section 2.2), on the fuel thermal conductivity. Thermal diffusivity data reported by Kinoshita *et al.* (2000) on irradiated fuel, obtained by a laser flash technique, indicate that the thermal diffusivity do not decrease appreciably beyond burnups of 70 MWd/kgU (close to the threshold burnup for fuel re-structuring).

The results reported by Kinoshita *et al.* are rather scanty (3 data points with no uncertainty analysis) for drawing definite conclusions on the impact of the rim zone on fuel thermal conductivity. However, some remarks can be made about the impact of the rim zone. The rim zone layer is usually 100-200 μm wide, with a porosity ranging between 10% and 20 %, and it contains fission product gases and liquids. Thus, the predominant material in the rim region is still the solid UO_2 material, which of course is irradiation-damaged and holds solid fission products, but is the chief contributor to the thermal conductivity.

It is worth recalling that the lattice thermal conductivity can be expressed by the formula $k = Cv\ell/3$, where C is the specific heat per unit volume, v is the velocity of lattice waves (sound) and ℓ is the mean free path of the phonon. Thermal diffusivity is the product $D_{th} = v\ell$, which is thus only a portion of the contribution to the thermal conductivity. Kinoshita *et al.* (2000) do not identify the contribution of the specific heat of the rim region to fuel thermal conductivity. Whether the specific heat of the restructured rim region is identical or higher than that of the unstructured UO_2 has not been analysed.

We should remark that the Debye's fundamental theory of thermal conductivity of solids gives a more precise relationship between conductivity and diffusivity, namely

$$k_{latt} = \frac{v}{3}\int_0^{\omega_D} C(\omega)\ell(\omega)d\omega, \tag{8}$$

where $C(\omega)d\omega$ is the specific heat per unit volume of lattice modes of frequency ω, and ω_D is the Debye frequency, see e.g. Dekker (1958). The inverse mean free path, or the scattering probability per unit path length $\ell(\omega)^{-1}$, is composed of individual interaction processes that are assumed to be additive and hence can be written as

$$\frac{1}{\ell(\omega)} = \frac{1}{\ell_i} + \frac{1}{\ell_d} + \frac{1}{\ell_p} + \frac{1}{\ell_b}. \tag{9}$$

Here, ℓ_i is the intrinsic phonon-phonon interaction mean free path due to lattice anharmonicity, ℓ_d scattering by point defects, ℓ_p scattering by extended imperfections such as pores or gas bubbles, and ℓ_b is scattering by grain boundaries, dislocations and other line-shaped defects, such as cracks. In the re-structured rim region, all these processes except ℓ_i are affected due to enhanced fissioning. For example, Klemens (1960) showed that $\ell_d^{-1} = A\omega^4$ where A is proportional to the defect concentration, $\ell_p^{-1} = n\sigma$, where n is the number per unit volume of pores and other extended defects and σ is the phonon-defect scattering cross section (Klemens, 1984). Finally, the boundary mean free path ℓ_b is of the order of the grain size.

Let us first estimate the contribution of ℓ_d in the rim region. Actually, in a theoretical analysis resting on Debye's theory, Klemens (1960) combined the contributions of point defect-phonon scattering and the anharmonic three-phonon processes (Umklapp processes) and then by using eq. (8) obtained a simple formula for the change in the lattice thermal resistance due to presence of point defects at high temperatures ($T > \Theta_D$, where Θ_D is the Debye temperature).

Writing Klemens's formula in terms of the factors in eq. (7), gives

$$k_{1d} = \frac{\omega_K}{\omega_D} \arctan\left(\frac{\omega_D}{\omega_K}\right), \tag{10}$$

where ω_K is the Klemens frequency, defined as $\ell_i(\omega_K) = \ell_d(\omega_K)$, which is a material property and may be determined from measurements. We have plotted relation (10) in figure 6.

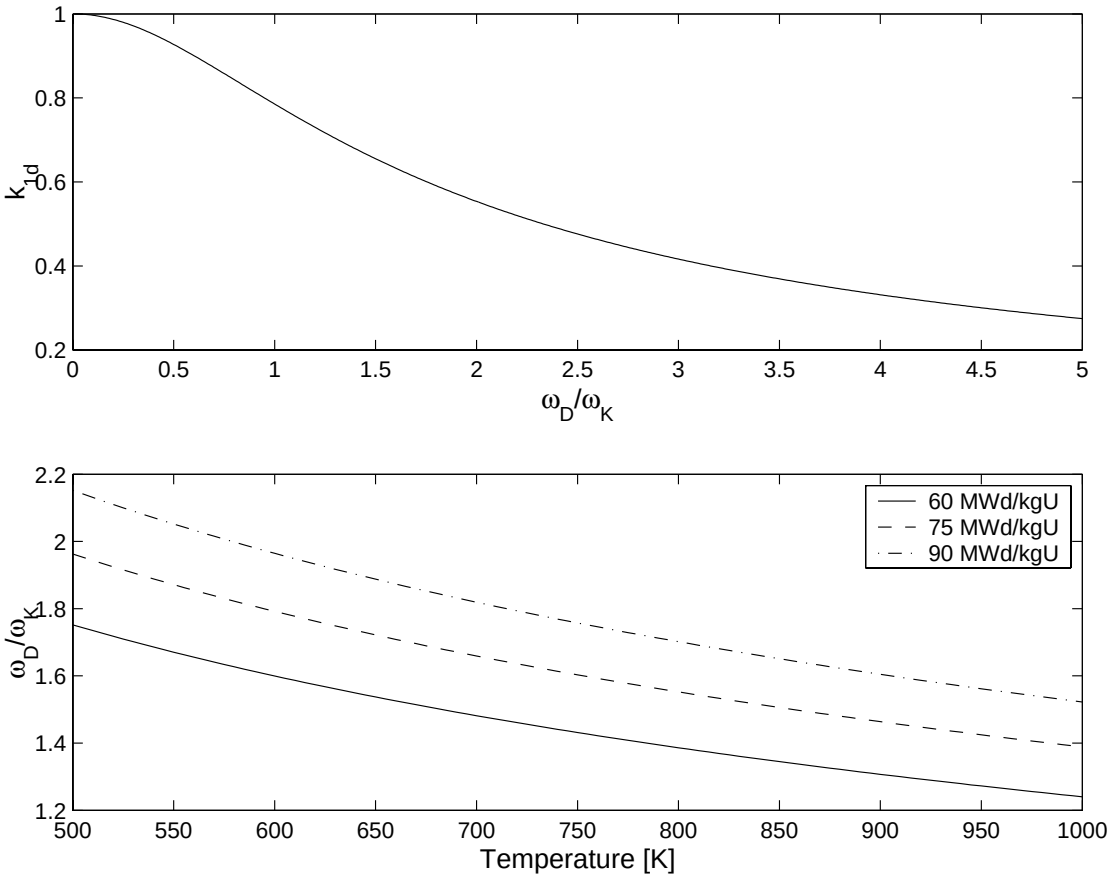

Figure 6: The upper figure shows a master curve for reduction in thermal conductivity due to the presence of point defects in a crystalline solid, where ω_D/ω_K is the ratio of the Debye frequency to the Klemens frequency, which is a measure of the intensity of defect-phonon scattering, eq. (10). The lower figure shows variation of ω_D/ω_K with temperature at several burnups, according to Lucuta et al.'s (1996) correlation obtained from thermal conductivity measurements on SIMFUEL.

We note that for the problem under consideration, *i.e.* highly irradiated nuclear fuel, we are interested in the case of strong point defect scattering, when $\ell_i(\omega_D) > \ell_d(\omega_D)$, *i.e.* for $\omega_D > \omega_K$. The Debye frequency is a basic property of crystalline solids. It is related to the Debye temperature according to $\omega_D = k_B \Theta_D / \hbar$, where k_B is the Boltzmann constant and $\hbar$ is the Planck constant. On the other hand, ω_K is a temperature-dependent parameter ($\omega_K \propto \sqrt{T}$), proportional to defect density and other material characteristics (Klemens, 1985).

Lucuta *et al*. (1994) and (1996) empirically determined ω_D/ω_K by fitting thermal conductivity data on SIMFUEL, using relation (10) and supposing the theoretical temperature variation of the form, $\omega_K/\omega_D \propto \sqrt{T}$. We have plotted their correlation as a function of temperature at a burnup of 8 at.% (75 MWd/kgU) in figure 6. From the figure, we may estimate the reduction in thermal conductivity in the rim re-structured region at T = 773 K, which gives, $\omega_D/\omega_K \approx 1.58$ and $k_{1d} \approx 0.64$, hence 36% reduction in thermal conductivity due to scattering by point defects in the re-structured fuel rim region.

Let us next consider the effect of rim zone porosity on ℓ_p. As discussed by Lucuta *et al*., the factor k_{1p} appearing in eq. (7), at T = 773 K (pellet rim temperature), has insignificant impact on thermal conductivity. We can therefore attempt to estimate the reduction in thermal conductivity due to rim zone formation by using the Maxwell expression for the factor k_{2p} appearing in eq. (7), namely $k_{2p} = (1-p)/(1+p/2)$. Assuming a porosity increase from 0.05 to p = 0.20, k_{2p} changes from 0.93 to 0.73, *i.e.* about 20% decrease in the thermal conductivity in the re-structured rim region relative to the material before re-structuring.

Finally, in regard to the influence of grain size on the thermal conductivity, we note that owing to a substantial grain subdivision in the rim region, we expect considerable reduction in ℓ_b. For example, if $\ell_b = 10\,\mu\text{m}$ in the original fuel (size of a grain), in the re-structured rim region $\ell_b \cong 0.2\,\mu\text{m}$. However, we realize that this is a rough order of magnitude estimate, since the details of ℓ_b is more convoluted than what we have offered here. Nevertheless, all the aforesaid theoretical assessments indicate that the thermal conductivity of the re-structured fuel rim region should decrease substantially, contrary to the preliminary results reported by Kinoshta *et al*. (2000).

To conclude the discussion on thermal conductivity, we have plotted four burnup-dependent correlations, reported in literature, as a function of temperature and burnup in figures 7a-d. These correlations are defined in appendices A-C. Figure 7a shows the correlation recommended by Lucuta *et al*. (1996) in the frame of eq. (7). Figures 7b-7c present the correlations suggested by Kosaka (1993) and Wiesenack *et al*. (1996), respectively, based on fuel central temperature measurements at the Halden heavy water BWR, and figure 7d depicts the correlation suggested by Ohira and Itagaki (1997). From these plots, we see that there are appreciable differences in the conductivity values, especially at lower temperatures and higher burnups. We note the peculiar behaviour of the correlation by Lucuta *et al*. at zero burnup. This is a manifestation of the irradiation-damage term, k_{4r}, in eq (7), which is assumed to be burnup independent, *i.e*. crystal damage occurs instantaneously under irradiation.

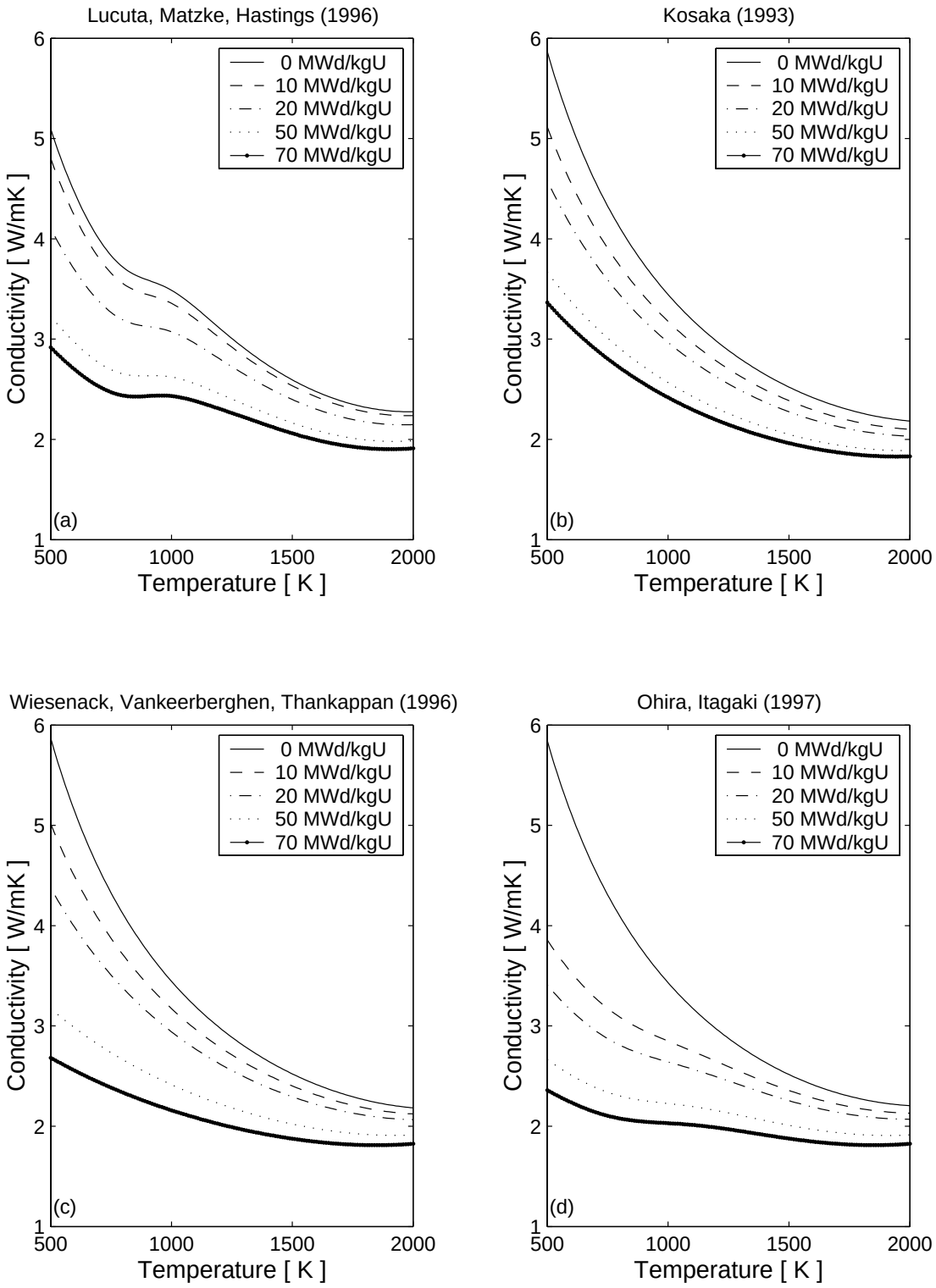

Figure 7: Thermal conductivity correlations for UO_2 fuel with respect to temperature and burnup. All correlations are plotted for 5% porosity (95% TD). (a) Lucuta et al. (1996); (b) Kosaka (1993) ; (c) Wiesenack et al. (1996); (d) Ohira and Itagaki (1997).

For neither of these fitted correlations, with the exception of Kosaka's, the authors provide uncertainty analysis, although there are considerable uncertainty and approximation in the inverse fitting procedures utilized. It is worth mentioning that a shortcoming with Kosaka's correlation is that the burnup-dependent term in the lattice conductivity is of a parabolic form: $h(u) = d_1 d_2 u(1 - d_2 u)$ where d_1 and d_2 are positive constants. This function has two zeros, $u = 0$ and $u = u_0 = d_2^{-1}$. Also, $h(u)$ has a maximum at $u = u_{\max} = 0.5 d_2^{-1}$. According to Kosaka, $d_2 \approx 4.37 \times 10^{-3}$ $(\text{MWd/kgU})^{-1}$, which means that $u_0 \approx 228$ and $u_{\max} \approx 114$ MWd/kgU.

Hence, thermal conductivity begins to *increase* for $u > u_{\max}$, which is an artefact of the fitting exercised. In contrast, the empirical correlations for h proposed by Wiesenack *et al*. (1996) and Ohira and Itagaki (1997) are monotonically increasing functions of burnup.

4 Analyses of rod DH in Halden IFA-429/519.9

4.1 Fuel rod design and irradiation conditions

The fuel rod considered in this analysis is one of three PWR rodlets, which were irradiated to an average burnup close to 100 MWd/kgU in the Halden heavy water reactor (Turnbull, 2001). The main purpose of the experiment was to investigate the effects of different fuel grain size and pellet-to-clad gap size on FGR, and hence, the three rodlets differed with respect to these parameters. The design of rod DH is summarized in table 3. In comparison with the other two rods, it had an unusually small-grained fuel.

Rod DH was first loaded into Halden Instrumented Fuel Assembly (IFA) 429, in which it was irradiated to an average burnup of 29 MWd/kgU. The rod average linear heat generation rate (LHGR) was below 20 kW/m, but the uppermost part of the rodlet experienced about 50% higher power, due to a pronounced upper-peaked axial power profile. After irradiation in IFA-429, the rod was re-instrumented with a pressure transducer, so that FGR could be monitored from changes in rod internal pressure during subsequent irradiation. The re-instrumented rod was loaded into IFA-519.9, in which it was subjected to significantly higher power levels than during previous irradiation. The complete power history for rod DH, comprising the irradiation both in IFA-429 and IFA-519.9, is shown in figure 8.

Unfortunately, due to leakage of helium from the rod, the in-core pressure measurements could not be used to determine FGR during the irradiation in IFA-519.9. However, it was assumed that the fission gases Xe and Kr, which are much heavier than helium, were retained in the fuel rod, and that the post-irradiation measurements of FGR through mass spectrometry are correct (Turnbull, 2001). The results of post-irradiation measurements are summarized in table 4, in which calculated values from our analysis with FRAPCON3 are included for comparison.

Fuel pellets			**Cladding**		
Material		UO_2	Material		Zr-4
Density	%TD	94.7	Inner diameter	mm	9.50
Grain size	μm	6.0	Outer diameter	mm	10.73
Enrichment ^{235}U	%	13.0			
Pellet diameter	mm	9.30	**Fill gas**		
Pellet height	mm	15.20	Composition		He
Active fuel length	mm	244	Gas pressure	MPa	2.5

Table 3: Design of rod DH.

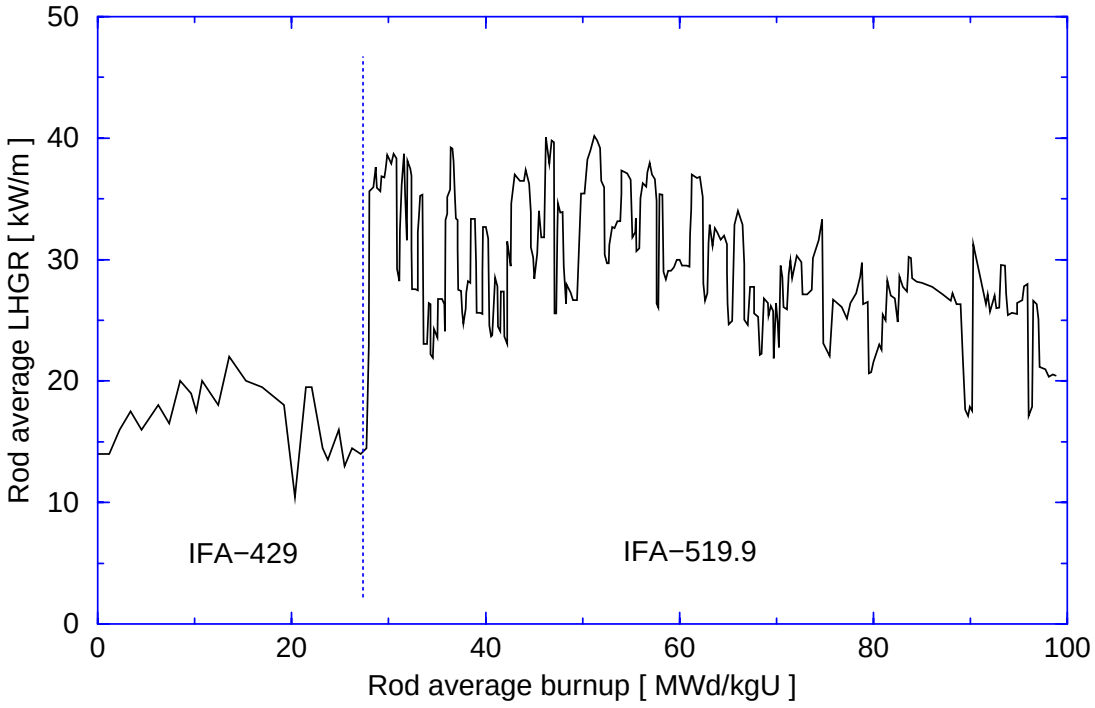

Figure 8: Power history for rod DH in IFA-429 and IFA-519.9. Data from Lanning et al. (1997) were used for irradiation in IFA-429, whereas data from Turnbull, (2001) were used for IFA-519.9.

4.2 Calculated fission gas behaviour

Figure 9 shows the fission gas release with respect to irradiation time calculated by FRAPCON3, both with standard models for FGR and with our modified models. The calculated results differ, but it is also noteworthy that the end-of-life fission gas release is underestimated by both sets of models. This can partly be due to the fact that the power history and axial power profile used in our analysis are approximate, and large errors are likely in applied fuel local power. Secondly, the observed leakage of helium is not considered in the calculations. The loss of helium is assumed to deteriorate pellet-to-clad heat transfer, thereby leading to higher fuel temperatures and enhanced thermal FGR.

Figure 10 shows the predicted radial distribution of retained fission gas at the peak burnup axial position (uppermost part) of rod DH at end of life, as calculated by our modified models for fission gas release. The radial distribution of totally produced fission gas is shown for comparison. The results show that the FGR is dominated by thermal release processes in the fuel central region. According to our analysis, 89.4% of the released gas was released by thermal processes. Figure 10 clearly shows that enhanced athermal fission gas release is predicted in the region $0.78 < r/r_p < 1$, where r_p is the fuel pellet radius. This region thus represents the rim zone, which in this case has a predicted width of $0.22r_p = 1.0$ mm. As shown in table 4, this value is close to the measured rim zone width.

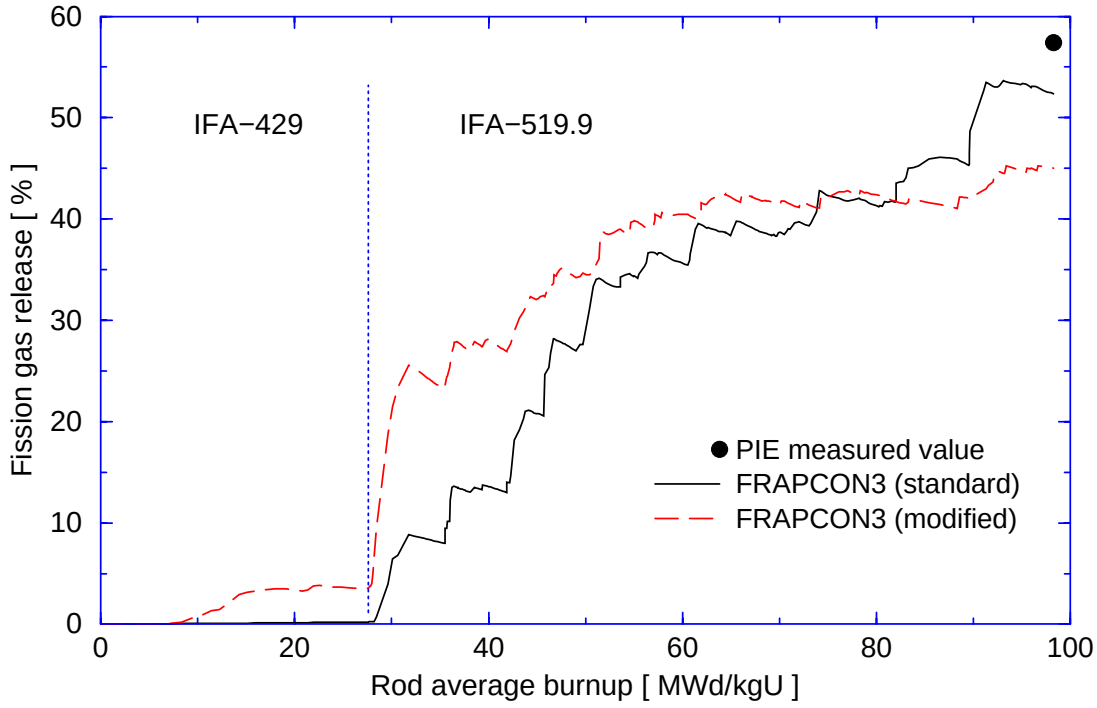

Figure 9: Fission gas release, calculated with the standard FRAPCON3 fission gas release models as well as the modified models described in sections 3.1 and 3.3. Measured value is shown for comparison.

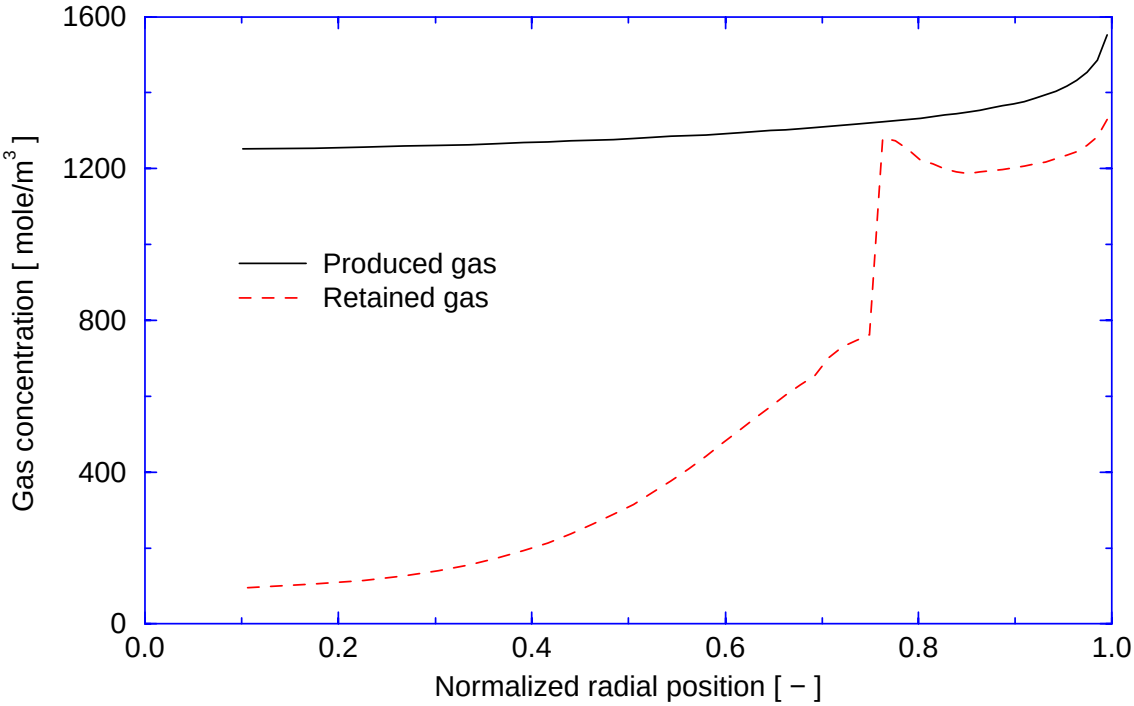

Figure 10: Predicted end-of-life radial distribution of retained fission gas in the peak burnup axial section. The distribution of produced gas is shown for comparison. A radial mesh consisting of 50 equal volume annuli was used in the analysis.

Figure 10 also shows that there is a thin annular region at $r/r_p \approx 0.76$, from which only a minor part of the produced fission gas is released through athermal processes. This region is also clearly visible in figure 11, which shows the calculated radial variation in the Xe/Kr-ratio of retained fission gas at end-of-life. Since gas produced throughout the entire irradiation history is contained within this region, it has a much lower Xe/Kr-ratio than the gas retained in regions from which much of the 'older' gas inventory has been released. The predicted Xe/Kr-ratio of gas within the rod plenum is 6.4, which is lower than the measured value of 7.2. The discrepancy could be due to underestimation of either the rim zone release or the thermal release under the final part of the irradiation history. Moreover, our fission gas release models do not consider possible radial migration and mixing of fission gases within the fuel pellet. As described in section 3.1, the models consider radial diffusion of gas atoms within individual grains, but not within the fuel pellet as a whole. A gas atom is thus assumed to remain at the pellet radial position at which it is created, until it is eventually released. To this end, it should be noticed that the calculations are based on the assumption of identical transport behaviour for Xe and Kr; *i.e.* identical effective diffusion coefficients and re-solution rates are assumed for these gases.

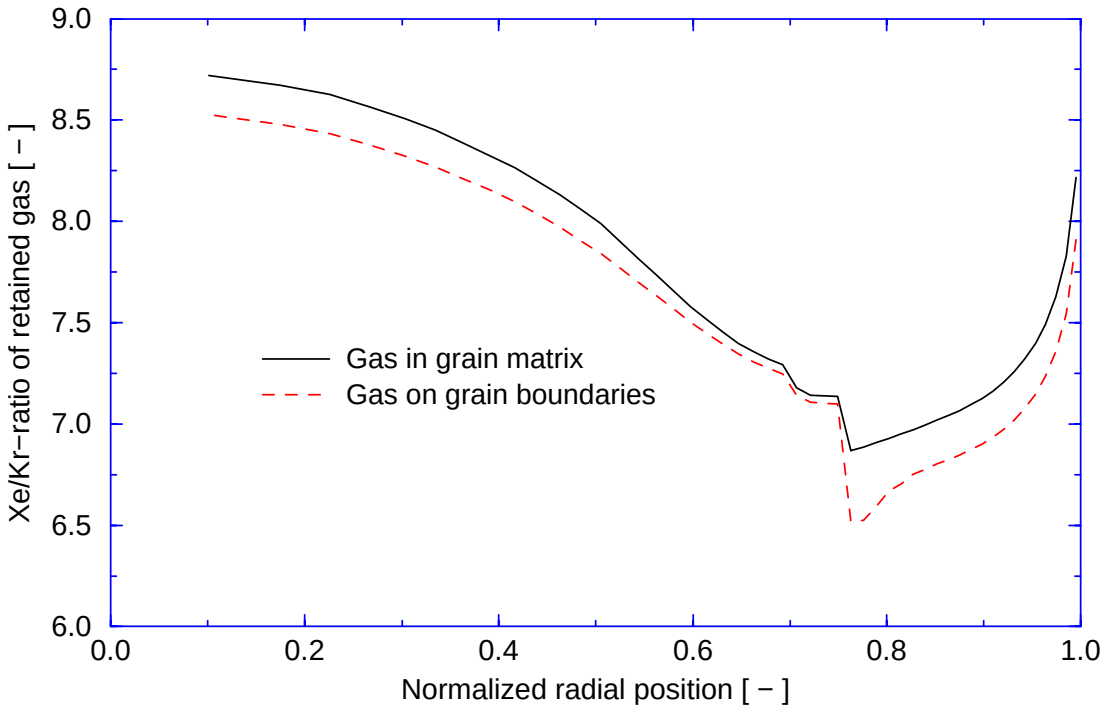

Figure 11: Predicted Xe/Kr-ratio of the gas retained in fuel grains and grain boundaries at end of life. The rod peak burnup axial section is considered. A radial mesh consisting of 50 equal volume annuli was used in the analysis

Parameter		Measured	Calculated
Rod average burnup	MWd/kgU	94.2	98.3
Fission gas release	%	57.4	45.0
Fission gas Xe/Kr-ratio	-	7.2	6.4
Rim zone width	mm	0.8-0.9	1.0

Table 4: Comparison of measured and calculated end-of-life fuel properties. The calculations were made by FRAPCON3, in which the modified models for fission gas release in sections 3.1 and 3.3 were used.

4.3 Influence of fuel thermal conductivity

The correlation for fuel thermal conductivity proposed by Lucuta *et al*. (1996) is the standard model in FRAPCON3, and it was used in the above analysis of rod DH in IFA-429/519.9. Recently, Lanning *et al*. (2000) evaluated this correlation by comparing FRAPCON3 predictions with in-reactor fuel temperature data from Halden, and found that it underpredicted the measured temperatures for pellet average burnups above 40 MWd/kgU. Moreover, they also implemented the correlations proposed by Wiesenack *et al.* (1996) and Ohira and Itagaki (1997) in FRAPCON3, and showed that these correlations gave significantly better fuel temperature predictions at high burnup than Lucuta's correlation.

We therefore analysed rod DH also with the latter two correlations, in order to study the effect of fuel thermal conductivity on fission gas release at high burnup. End-of-life conditions, which were calculated by FRAPCON3 with the modified models for fission gas release and each of the three different correlations for fuel thermal conductivity, are compared in table 5. Evidently, both the calculated end-of-life fuel temperature and fission gas release are significantly influenced by the applied correlation for thermal conductivity. However, the Xe/Kr-ratio is underestimated for all cases, irrespective of the large changes in thermal release fractions. This would indicate that the comparatively high measured Xe/Kr-ratio in IFA-429/519.9 is due to athermal release processes from the rim zone. An alternative explanation could be that the high Xe/Kr-ratio in rod DH is caused by leakage of krypton, which due to its lower atomic weight and superior mobility has a higher probability to escape from the rod than xenon.

End-of-life conditions		Measured value	Calculations with modified FRAPCON3		
			Lucuta *et al*. (1996)	Wiesenack *et al.* (1996)	Ohira & Itagaki (1997)
Total FGR	%	57.4	45.0	50.2	53.0
Thermal FGR	%	-	40.2	45.7	48.9
Athermal FGR	%	-	4.8	4.5	4.1
Xe/Kr-ratio	-	7.2	6.41	6.46	6.47
Fuel peak temp.	K	-	1333	1458	1494

Table 5: Calculated EOL conditions, when different correlations for fuel thermal conductivity are used in FRAPCON3.

5 Summary and conclusions

Among the numerous phenomena that may affect fission gas release from high-burnup UO_2 nuclear fuel, most attention is usually given to the rim zone formation and its effect on athermal fission gas release. This is understandable, since formation of the porous, small-grained microstructure close to the pellet surface at a local burnup of 60-70 MWd/kgU is clearly connected with a simultaneous enhancement of athermal fission gas release. Although the underlying mechanisms for this enhancement are as yet unclear, it seems that part of it is connected with release of retained gas as an immediate effect of grain re-structuring, whereas another part stems from an increased steady-state release rate from the re-structured material. The increased steady-state release rate is attributed to an increase in the fuel specific surface (open porosity) and/or to irradiation-enhanced athermal diffusion in the porous and small-grained rim zone material.

In addition to these strictly athermal effects, one must also consider the potential for thermal fission gas release at extended fuel burnup. This is a complicated matter, since the fuel temperature is affected by several interacting high-burnup phenomena, such as pellet-clad gap closure, fission gas contamination of the gap, changes in radial distribution of fissile material, and last but not least, fuel thermal conductivity degradation.

The thermal conductivity degradation is primarily caused by an increased resistance to phonon heat transport, as irradiation damage and fission products accumulate in the crystal lattice. Theoretical models for thermal conductivity of solids, by which the effects of porosity, grain size and lattice defects can be evaluated, indicate that the thermal conductivity should decrease substantially in the fuel rim zone as a consequence of grain subdivision and increased porosity.

In an attempt to study the relative importance of various phenomena to the integral fission gas release behaviour at high burnup, we analysed rod DH in the Halden IFA-429/519.9 experiment by use of the FRAPCON3 computer code. Since the standard model for thermal fission gas release in FRAPCON3 performed poorly for low release fractions, it was replaced with a modified model. The modifications primarily concerned modelling of gas atom re-solution from grain boundaries and the effect of pellet hydrostatic stress on grain boundary gas saturation, but also the applied correlation for the gas diffusion coefficient was altered. Moreover, we also replaced the FRAPCON3 standard model for rim zone fission gas release, which consists of a simple correlation between athermal release and pellet average burnup. In our model, rim zone fission gas release is calculated with consideration of the radial distributions of burnup, retained fission gas and temperature close to the pellet periphery. In our modified models, xenon and krypton were treated as individual gas species under both production and release, which made it possible to calculate the Xe/Kr-ratio of gas retained within grains, gas accumulated in grain boundary bubbles, and gas released to the rod free volume.

Unfortunately, there was an appreciable (>50%) leakage of helium from rod DH at some stage in the irradiation of IFA-519.9, which complicates analyses of the experiment. Neglecting this loss of helium, the fission gas release fraction calculated by our modified version of FRAPCON3 falls below the measured data, although the calculated fission gas release depends strongly on what correlation is used for fuel thermal conductivity. Empirical correlations, formulated on the basis of in-reactor fuel centre temperature measurements, give better agreement with measured data from the IFA-429/519.9 experiment than the theoretically based correlation by Lucuta *et al.* (1996). This is in agreement with results from a similar study, performed by Lanning *et al*. (2000).

The fission gas release in rod DH is dominated by thermal release processes, and according to our calculations, athermal mechanisms account for less than 10% of the total fission gas release. The calculated Xe/Kr-ratio is below the measured value, which could be due to either underestimation of athermal fission gas release from the rim zone, or escape of krypton from the leaking rod during irradiation.

6 References

Barner, J.O., Cunningham, M.E., Freshley, M.D. and Lanning, D.D., 1993.
Evaluation of fission gas release in high-bunup light water reactor fuel rods,
Nucl. Technology 102, pp 210-231.

Berna, G.A., Beyer, C.E., Davies, K.L. and Lanning, D.D., 1997.
FRAPCON3: A computer code for the calculation of steady-state, termal-mechanical behavior of oxide fuel rods for high burnup, U.S. Nuclear Regulatory Commission Report NUREG/CR-6534, Volume 2, December 1997.

Bernard, L.C., Jacoud, J.L. and Vesco, P., 2002.
An efficient model for the analysis of fission gas release, J. Nucl. Mat. 302, pp 125-134.

Bråten, K. and Minagawa, Y., 1999.
Review of Halden data on axial gas transport in operating fuel rods,
OECD Halden Reactor Project Report HWR-617, Halden, Norway.

Decker, A.J., 1958.
Solid state physics, MacMillan and Company, London, 1958.

Dowling, D.M., White, R.J. and Tucker, M.O., 1982.
The effect of irradiation-induced re-solution on fission gas release,
J. Nucl. Mat. 110, pp 37-46.

Duderstadt, J.J. and Hamilton, L.J., 1976.
Nuclear reactor analysis, John Wiley & Sons, New York, Chap. 2.

Forsberg, K., Lindström, F. and Massih, A.R., 1994.
Modelling of some high burnup phenomena in nuclear fuel, Proc. IAEA Technical Committee Meeting on nuclear fuel behaviour modeling at high burnup and its experimental support, September 19-23, Windermere, UK, 1994.

Forsberg, K. and Massih, A.R., 1985.
Diffusion theory of fission gas migration in irradiated nuclear fuel UO_2,
J. Nucl. Mat. 135, pp 140-148.

Hagrman, D.L. and Reymann, G.A., 1979.
MATPRO Version 11: A handbook of materials properties for use in the analysis of light water reactor fuel behavior, NUREG Report CR-0497.

Harding, J.H. and Martin, D.G., 1989.
A recommendation for thermal conductivity of UO_2, J. Nucl. Mat. 166, pp 223-226.

Hyland, G.H., 1983.
Thermal conductivity of solid UO_2: critique and recommendation,
J. Nucl. Mat. 113, pp 125-132.

Kameyama, T., Matsumura, T. and Kinoshita, M., 1994.
Numerical analysis for microstructure change of a light water reactor fuel pellet at high burn-up, Nucl. Technology 106, pp 334-341.

Kashibe, S., Une, K. and Nogita, K., 1993.
Formation and growth of intragranular fission gas bubbles in UO_2 fuels with burnup of 8-63 GWd/t, J. Nucl. Mat. 206, pp 22-34.

Kinoshita, M., Sonoda, T., Kitajima, S., Sasahara, A., Kolstad, E., Matzke, Hj., Rondinella, V.V., Stalios, A.D., Walker, C.T., ray, I.L.F., Scheindlin, M., Halton, D. and Ronchi, C., 2000.
High burnup rim project (II): Irradiation and examination to investigate rim-structured fuel, Proc. ANS Topical Meeting on Light Water Reactor Fuel Performance, Park City, Utah, April 10-13, 2000.

Klemens, P.G., 1960.
Thermal resistance of point defects at high temperatures,
Physical Review 119, pp 507-509.

Klemens, P.G., 1984.
Theory of thermal conduction in dielectric solids: effect of radiation damage,
Nucl. Instruments and Meth. in Physics Research B1, pp 204-208.

Klemens, P.G., 1985.
Theory of heat conduction in nonstoichiometric oxides and carbides,
High Temperatures High Pressures, 17, pp 41-45.

Kogai, T., 1997.
Modelling of fission gas release and gaseous swelling of light water reactor fuels,
J. Nucl. Mat. 244, pp 131-140.

Kogai, T., Ito, K. and Iwano, Y., 1988.
The effect of cladding restraint on fission gas release behavior,
J. Nucl. Mat. 158, pp 67-70.

Kosaka, Y., 1993.
Thermal conductivity degradation analysis of the ultra high burnup experiment IFA-562, OECD Halden Reactor Project Report HWR-341, Halden, Norway.

Lanning, D.D., Beyer, C.E. and Berna, G.A., 1997.
FRAPCON3: Integral assessment, U.S. Nuclear Regulatory Commission Report NUREG/CR-6534, Volume 3, December 1997.

Lanning, D.D., Beyer, C.E. and Cunningham, M.E., 2000.
FRAPCON-3 fuel rod temperature predictions with fuel conductivity degradation caused by fission products and gadolinia additions, Proc. ANS Topical Meeting on Light Water Reactor Fuel Performance, Park City, Utah, April 10-13, 2000.

Lassmann, K., O'Carroll, C., van de Laar, J. and Walker, C.T., 1994.
The radial distribution of plutonium in high burnup UO_2 fuels,
J. Nucl. Mat. 208, pp 223-231.

Lassmann, K., Schubert, A., van de Laar, J. and Vennix, C.W.H.M., 2000.
Recent developments of the TRANSURANUS code with emphasis on high burnup phenomena, Proc. IAEA Technical Committee Meeting on nuclear fuel behaviour modeling at high burnup and its experimental support, June 19-23, Windermere, UK, 2000.

Lemoine, F., Papin, J., Frizonnet, J-M., Cazalis, B. and Rigat, H., 2000.
The role of grain boundary fission gases in high burn-up fuel under reactivity initiated accident conditions, Proc. of OECD Nuclear Energy Agency seminar on fission gas behaviour in water reactor fuels, September 26-29, Cadarache, France.
ISBN 92-64-19715-X.

Lucuta, P.G., Matzke, Hj. and Hastings, I.J., 1996.
A pragmatic approach to modelling thermal conductivity of irradiated UO_2 fuel: review and recommendations, J. Nucl. Mat. 232, pp 166-180.

Lucuta, P.G., Matzke, Hj. and Verrall, R.A., 1994.
Modelling of UO_2-based SIMFUEL thermal conductivity: the effect of burnup,
J. Nucl. Mat. 217, pp 279-286.

Lösönen, P., 2000.
On the behaviour of intragranular fission gas in UO_2 fuel,
J. Nucl. Mat. 280, pp 56-72.

Manzel, R. and Coquerelle, M., 1997.
Fission gas release and pellet structure at extended burnup,
Proc. ANS Topical Meeting on Light Water Reactor Fuel Performance, Portland, Oregon, March 2-6, 1997, pp 463-470.

Matzke, Hj., 1995.
The rim-effect in high burnup UO_2 nuclear fuel,
In P. Vincenzini (ed), Ceramics: Charting the Future, Proc. World Ceramics Congress, Florence, Italy, June 28 - July 4, pp 2913-2920.

Mogensen, M., Bagger, C. and Walker, C.T., 1993.
An experimental study of the distribution of retained xenon in transient-tested UO_2 fuel,
J. Nucl. Mat. 199, pp 85-101.

Mogensen, M., Pearce, J.H. and Walker, C.T., 1999.
Behaviour of fission gas in the rim region of high burn-up UO_2 fuel pellets with particular reference to results from an XRF investigation, J. Nucl. Mat. 264, pp 99-112.

Nakamura, J., Suzuki, M. and Uetsuka, H., 1999.
Re-irradiation tests of LWR spent fuel at JMTR, Proc. EHPG meeting, May 24-29, Loen, Norway. OECD Halden Reactor Project Report HPR-351, Volume 1, Halden, Norway.

Nogita, K. and Une, K., 1994.
Radiation-induced microstructural change in high burnup UO_2 fuel pellets, Nucl. Instruments and Meth. in Physics Research B91, pp 301-306.

Noirot, J., Desgranges, L. and Marimbeau, P., 2000.
Contribution of the rim to the overall fission gas release: What do isotopic analyses reveal? Proc. of OECD Nuclear Energy Agency seminar on fission gas behaviour in water reactor fuels, September 26-29, Cadarache, France. ISBN 92-64-19715-X.

Ohira, K. and Itagaki, N., 1997.
Thermal conductivity measurements of high burnup UO_2 pellet and a benchmark calculation of fuel center temperature, Proc. ANS Topical Meeting on Light Water Reactor Fuel Performance, Portland, Oregon, March 2-6, 1997, pp 541-549.

Olander, D.R., 1976.
Fundamental aspects of nuclear reactor fuel elements, U.S. Department of Energy, ISBN 0870790315.

Palmer, I.D., Hesketh, K.W. and Jackson, P.A., 1983.
A model for predicting the radial power profile in a fuel pin, In J. Gittus (ed) Water Reactor Fuel Element Performance Computer Modelling, Applied Science, Barking, UK.

Rest, J. and Hofman, G.L., 1995.
Effect of recrystallization in high-burnup UO_2 on gas release during RIA-type transients, J. Nucl. Mat. 223, pp 192-195.

Rest, J. and Hofman, G.L., 1994.
Dynamics of irradiation-induced grain subdivision and swelling in U_3Si_2 and UO_2 fuels, J. Nucl. Mat. 210, pp 187-202.

Sontheimer, F. and Landskron, H., 2000.
Puzzling features of EPMA radial fission gas release profiles: The key to realistic modeling of fission gas release up to ultra high burnup of 100 MWd/kgM with CARO-E, Proc. IAEA Technical Committee Meeting on nuclear fuel behaviour modeling at high burnup and its experimental support, June 19-23, Windermere, UK, 2000.

Speight, M.V., 1969.
A calculation of the migration of fission gas in material exhibiting precipitation and re-solution of gas atoms under irradiation, Nucl. Sci. Eng. 37, pp 180-185.

Spino, J., Vennix, K. and Coquerelle, M., 1996.
Detailed characterization of the rim microstructure in PWR fuels in the burn-up range 40-67 GWd/tM, J. Nucl. Mat. 231, pp 179-190.

Thomas, L.E., Beyer, C.E. and Charlot, L.A., 1992.
Microstructural analysis of LWR spent fuels at high burnup,
J. Nucl. Mat. 188, pp 80-89.

Turnbull, J.A., 1999.
An assessment of fission gas release and the effect of microstructure at high burn-up,
OECD Halden Reactor Project Report HWR-604, Halden, Norway.

Turnbull, J.A., 2001.
Concluding report on three PWR rods irradiated to 90 MWd/kgUO_2 in IFA-519.9: Analysis of measurements obtained in-pile and by PIE, OECD Halden Reactor Project Report HWR-668, Halden, Norway.

Turnbull, J.A., 2002.
The high burn-up restructuring of fuel, the so called rim effect: A consideration of its impact on steady-state and transient behaviour, OECD Halden Reactor Project Report HWR-709, Halden, Norway.

Une, K., Nogita, K., Kashibe, S., Toyonaga, T. and Amaya, M., 1997.
Effect of irradiation-induced microstructural evolution on high burnup fuel behaviour,
Proc. ANS Topical Meeting on Light Water Reactor Fuel Performance, Portland, Oregon, March 2-6, 1997, pp 478-489.

Une, K., Nogita, K., Suzawa, Y., Hayashi, K., Ito, K. and Etoh, Y., 2000.
Effects of grain size and PCI restraint on the rim structure formation of UO_2 fuels,
Proc. ANS Topical Meeting on Light Water Reactor Fuel Performance, Park City, Utah, April 10-13, 2000.

Vitanza, C., Kolstad, E. and Graziani, V., 1979.
Analysis of fission gas release tests to high burnup,
Proc. ANS Topical Meeting on Light Water Reactor Fuel Performance, Portland, Oregon, April 29 – May 3, 1979.

Walker, C.T., 1999.
Assessment of the radial extent and completion of recrystallization in high burn-up UO_2 nuclear fuel by EPMA, J. Nucl. Mat. 275, pp 56-62.

White, R.J., 1994.
A new mechanistic model for the calculation of fission gas release, Proc. ANS Topical Meeting on Light Water Reactor Fuel Performance, West Palm Beach, Florida, April 17-21, 1994.

White, R.J., 2000.
Fission gas release, OECD Halden Reactor Project Report HWR-632, Halden, Norway.

Wiesenack, W., Vankeerberghen, M. and Thankappan, R., 1996.
Assessment of UO_2 thermal conductivity degradation based on in-pile temperature data,
OECD Halden Reactor Project Report HWR-469, Halden, Norway.

Appendix A:

UO_2 fuel thermal conductivity correlation by Lucuta *et al.*

In the model by Lucuta *et al*. (1996), the fuel thermal conductivity, k, is correlated to the local temperature, burnup, stoichiometry and porosity through

$$k = k_0 k_{1d} k_{1p} k_{2p} k_{3x} k_{4r} . \quad \text{(A1)}$$

Here, k_0 is the conductivity of unirradiated, fully dense fuel, k_{1d} and k_{1p} are burnup dependent corrections for dissolved and precipitated fission products in the fuel matrix, k_{2p} is a correction factor for fuel porosity, k_{3x} refers to the dependence on fuel stoichiometry, and k_{4r} is a temperature dependent compensation factor for irradiation effects. The conductivity of unirradiated fully dense fuel is calculated from a model given by Harding and Martin (1989)

$$k_0 = \frac{10000}{375 + 2.165T} + \frac{4.715 \times 10^9}{T^2} e^{-16361/T} , \quad \text{(A2)}$$

where T is the temperature in Kelvin and k_0 is in units of W/mK. The effects of dissolved and precipitated fission products on the conductivity are modeled by

$$k_{1d} = \left(\frac{1.09}{B^{3.265}} + \frac{0.0643\sqrt{T}}{\sqrt{B}} \right) \arctan\left(\left(\frac{1.09}{B^{3.265}} + \frac{0.0643\sqrt{T}}{\sqrt{B}} \right)^{-1} \right) \quad \text{(A3)}$$

and

$$k_{1p} = 1 + \left(\frac{0.019B}{3 - 0.019B} \right) \left(1 + e^{\frac{1200-T}{100}} \right)^{-1} , \quad \text{(A4)}$$

where B is the fuel local burnup in atom% (1 atom% corresponds to 9.383 MWd/kgU at 200 MeV/fission). The effect of fuel porosity is accounted for by the Maxwell factor

$$k_{2p} = \frac{1 - p}{1 + 0.5p} , \quad \text{(A5)}$$

where p is the volume fraction of porosity, stemming from fabrication and gaseous swelling.

The correction factor for fuel stoichiometry, k_{3x}, is unity for stoichiometric UO_2, *i.e.* for an oxygen-to-metal ratio (OM) of 2.

Irradiation decreases the fuel thermal conductivity at temperatures below 900-1000 K, and this effect is taken into account by the factor k_{4r}

$$k_{4r} = 1 - 0.2\left(1 + e^{\frac{T-900}{80}}\right)^{-1}. \qquad \text{(A6)}$$

It should be noticed, that this factor is applied at all times in the model, also for fresh fuel at zero burnup.

Appendix B:

UO_2 fuel thermal conductivity correlations by Kosaka and Wiesenack *et al.*

In the correlations by Kosaka (1993) and Wiesenack *et al.* (1996), the fuel thermal conductivity is correlated to the local temperature and burnup. For a fuel material with 5% porosity (95% TD), both correlations can be written as

$$k_{95} = \frac{1}{4.724 \cdot 10^{-2} + 2.475 \cdot 10^{-4} T + h} + 7.90 \cdot 10^{-3} e^{1.88 \cdot 10^{-3} T} . \quad \text{(B1)}$$

Here, T is the fuel temperature in Kelvin, and h is a burnup-dependent function, which differs between the two correlations. In the correlation by Kosaka, h is given by

$$h(u) = 2.641 \cdot 10^{-3} u - 1.153 \cdot 10^{-5} u^2 , \quad \text{(B2)}$$

whereas in the correlation by Wiesenack *et al.,* h also depends on temperature through

$$h(u,T) = \left(3.274 \cdot 10^{-3} - 7.042 \cdot 10^{-7} T \right) u . \quad \text{(B3)}$$

Here, u is the fuel burnup in MWd/kgU.

It should be noticed that equation (B1) originates from the MATPRO library of material properties (Hagrman and Reymann, 1979), into which the function h has been added as a burnup dependent correction factor by Kosaka and Wiesenack *et al*. For application of the above correlations to fuel materials with volume fractions of porosity, p, other than 0.05, a correction factor according to

$$k = k_{95} \frac{1 - \beta p}{1 - \beta 0.05} \quad \text{(B4)}$$

is applied, where

$$\beta = 2.738 - 5.8 \cdot 10^{-4} T . \quad \text{(B5)}$$

Appendix C:

UO_2 fuel thermal conductivity correlation by Ohira and Itagaki

The correlation by Ohira and Itagaki (1997) is similar in form to the correlations presented in appendix B. For a fuel material with 5% porosity (95% TD), the thermal conductivity is

$$k_{95} = \frac{1}{4.52 \cdot 10^{-2} + 2.46 \cdot 10^{-4} T + h} - 5.47 \cdot 10^{-9} T^2 + 2.29 \cdot 10^{-14} T^4. \quad \text{(C1)}$$

Here, T is the fuel temperature in Kelvin, and h is a burnup-dependent correction factor, which is given by

$$h(u,T) = 1.87 \cdot 10^{-3} u + \frac{3.8 \cdot 10^{-2} u^{0.28}}{1 + 396 e^{-6380/T}}, \quad \text{(C2)}$$

Here, u is the fuel burnup in MWd/kgU. For application of the above correlation to fuel materials with volume fractions of porosity, p, other than 0.05, a correction factor according to

$$k = k_{95} \frac{1 - \beta p}{1 - \beta 0.05} \quad \text{(C3)}$$

is applied. In this case, $\beta = 2.5$.